

CZECH TECHNICAL UNIVERSITY IN PRAGUE

FACULTY OF MECHANICAL ENGINEERING  
DEPARTMENT OF PROCESS ENGINEERING



INVESTIGATION OF THE TEST SECTION OF A  
SMALL WIND TUNNEL

MASTER THESIS

2019

TUGSAN ALAV



# MASTER'S THESIS ASSIGNMENT

## I. Personal and study details

Student's name: **Tugsan Alav** Personal ID number: **473132**  
Faculty / Institute: **Faculty of Mechanical Engineering**  
Department / Institute: **Department of Process Engineering**  
Study program: **Mechanical Engineering**  
Branch of study: **Process Engineering**

## II. Master's thesis details

Master's thesis title in English:

**Investigation of the test section of a small wind tunnel**

Master's thesis title in Czech:

**Vyšetřování zkušebního úseku malého větrného tunelu**

Guidelines:

The aim of the thesis is calculation and analysis of pressure and velocity field in an area after the diffuser in a test section of a wind tunnel. The fields shall be calculated with use of a CFD software for two cases. The first case will be open diffuser outlet. The second case will be with grids inserted to the outlet of the diffuser. The student shall also evaluate the formation of the boundary layer and design a measure for its minimization. The research part shall focus on the small closed wind tunnels, on the velocity and pressure field calculation and on the boundary layer formation. The geometry of the wind tunnel will be given.

Bibliography / sources:

Elofsson, P. 'KTH Vehicle Aerodynamics' Fluid Mechanics, 2004  
Olander, M. 'CFD of the Volvo Wind Tunnel' Master Thesis, 2011, Chalmers University

Name and workplace of master's thesis supervisor:

**Ing. Michal Netušil, Ph.D., Department of Process Engineering, FME**

Name and workplace of second master's thesis supervisor or consultant:

Date of master's thesis assignment: **23.04.2019** Deadline for master's thesis submission: **07.06.2019**

Assignment valid until: \_\_\_\_\_

Ing. Michal Netušil, Ph.D.  
Supervisor's signature

prof. Ing. Tomáš Jirout, Ph.D.  
Head of department's signature

prof. Ing. Michael Valášek, DrSc.  
Dean's signature

## III. Assignment receipt

The student acknowledges that the master's thesis is an individual work. The student must produce his thesis without the assistance of others, with the exception of provided consultations. Within the master's thesis, the author must state the names of consultants and include a list of references.

**30-04-2019**

Date of assignment receipt

  
Student's signature

# Annotation sheet

**Name:** Tugsan

**Surname:** Alav

**Title Czech:** Vyšetřování zkušebního úseku malého větrného tunelu

**Title English:** Investigation of the test section of a small wind tunnel

**Scope of work:** number of pages: 63

number of figures: 48

number of tables: 19

**Academic year:** 2018/2019

**Language:** English

**Department:** Process Engineering

**Specialization:** Process Technology

**Supervisor:** Ing. Michal Netusil, Ph.D.,

**Reviewer:**

**Tutor:**

**Submitter:** Czech Technical University in Prague, Faculty of Mechanical Engineering, Department of Process Engineering

**Annotation - Czech:** Cílem práce je výpočet a analýza tlakového a rychlostního pole v prostoru za ústím difuzoru v testovací části větrného tunelu. Pole mají být počítány za pomoci softwaru CFD pro dva případy. První případ je otevřené ústí difuzoru. Druhý případ je s mřížkami vloženými do ústí difuzoru. Student také vyhodnotí tvorbu mezní vrstvy a navrhne opatření pro její minimalizaci. Rešeršní část se zaměří na malé uzavřené větrné tunely, na výpočet rychlosti a tlaku a na formování mezní vrstvy. Geometrie větrného tunelu bude dána.

**Annotation - English:** The aim of the thesis is calculation and analysis of pressure and velocity field in an area after nozzle in a test section of a wind tunnel. The fields shall be calculated with use of a CFD software for two cases. The first case will be open nozzle outlet. The second case will be with grids inserted to the outlet of the nozzle. The research part shall focus on the small closed win tunnel which is designed by researcher with on the velocity, pressure field calculation and on the boundary layer formation. The geometry parameters will be given for designing.

**Keywords:** Nozzle, fluent, wind tunnel, pressure profile, velocity profile, boundary layer

**Utilization:** For Department of Process Engineering, Czech Technical University in Prague

**Declaration**

I confirm that the master's thesis was disposed by myself and independently, under the leading of my thesis supervisor. I stated all sources of the documents and literature.

In Prague... 06/06/2019 .....

A handwritten signature in black ink, consisting of a stylized, cursive-like script, positioned above a horizontal dotted line.

Name and Surname

# Acknowledgment

I take this opportunity to express my sincerest gratitude to Ing. Michal Netušil, Ph.D., for showing me the way and being there by my side at all the crucial moments throughout project work.

I also would like to thank prof. Ing. Jirí Nožička and Mehmet Ayaş for their kind cooperation and guidance in this project.

I am thankful of the Process engineering department, all of masters for them help in the project.

# Abstract

The wind tunnel is considered as an important device to test the aerodynamic performance of the different bodies. The wind tunnel performance depends on the characteristic of the air stream passing through the test section, and the aim of this research is to investigate pressure, velocity boundary conditions, and compressibility, incompressibility situations within the fully developed isentropic flow. Due to the specified maximum velocity of 50 m/s and subsonic flow located at the exit of the nozzle, the new nozzle geometry was designed. For the design hyperbolic analytical geometry equations and combination of the equation of motion, Mach number, and specific heat ratio were used. After that, a normal grid and a cylindrical grid were assembled at the exit of the nozzle to inspect changes at a car position (3 meters from the exit of the nozzle). The comparison of the theoretical results of pressures, velocities and density changes with the results of the Dynamic Gas table and Ansys Fluent analysis is performed.

# List of content

- List of content .....1**
- CHAPTER 1-INTRODUCTION .....3**
- Description of the Subsonic Wind Tunnel.....3**
- 1. What is the wind tunnel .....3
- 1.1Description of the Wind Tunnel.....3
- CHAPTER 2-LITERATURE RESEARCH .....4**
- FUNDAMENTAL OF FLUID MECHANICS FOR LOW-SPEED WIND TUNNELS.....4**
- 2.1 Boundary Layer .....4
- 2.2 The Continuity Equation .....5
- 2.3 Bernoulli Equation .....6
- 2.3.1 Darcy-Welsbach.....7
- 2.4 Reynold’s and Mach number .....7
- 2.4.1 Fluid, Flow and Reynold’s number .....8
- 2.4.2 Mach Number.....8
- CHAPTER 3 .....12**
- DESIGNING THE LOW-SPEED WIND TUNNEL.....12**
- 3.1 Wind Tunnel classification .....12
- 3.1.1 Closed Loop Wind tunnel.....12
- 3.2 Theory of Specific design .....13
- 3.2.1 Subsonic De-Laval nozzle .....13
- Theoretical description of De-Laval nozzle .....14
- Mass Conversation .....18
- Exit Velocity of Nozzle .....20
- 3.2.2 Geometry description of the test section .....21
- 3.3 Description of specific heat ratio of air .....10
- CHAPTER 4-PRACTICAL PART .....23**
- ANALYTICAL CALCULATIONS.....23**
- 4.1 De-Laval nozzle measurements calculation .....23
- 4.1.1 Temperature, Pressure, Density ratio and Exit, Inlet velocity in De-Laval nozzle .....26

4.1.2 Demonstration of analytical calculations by The Gas Dynamic Table; .....	28
4.1.3 Mass flow rate of the system and outlet velocity of the test section .....	30
4.1.4 Hydraulic diameter and Reynold's number at Critical location .....	31
<b>CHAPTER 5.....</b>	<b>33</b>
<b>MODEL OF GEOMETRY.....</b>	<b>33</b>
<b>CHAPTER 6.....</b>	<b>36</b>
<b>ANALYSIS OF THE SYSTEM.....</b>	<b>36</b>
6.1 Preparation for analysis.....	36
6.1.1 Geometry Preparation.....	37
6.1.2 Mesh.....	37
6.1.3 Fluent Solver.....	41
6.1.4 Pressure and Velocity Profile of the system.....	43
6.2 Grid Analysis.....	44
6.2.1 Model of Grid .....	45
6.2.2 Mesh of the model with a grid.....	45
6.2.3 Fluent Solver.....	46
6.3 Pipe (cylinder) Grid Analysis .....	49
6.3.1 Model of Pipe Grid.....	49
6.3.2 Mesh model of the cylinder(pipe) grid .....	49
6.3.3 Fluent Solver.....	50
<b>RESULTS AND DISCUSSION.....</b>	<b>53</b>
<b>NOMENCLATURE.....</b>	<b>59</b>
<b>REFERENCES.....</b>	<b>61</b>
<b>List of Figures.....</b>	<b>63</b>
<b>List of Tables.....</b>	<b>64</b>



# CHAPTER 1-INTRODUCTION

## Description of the Subsonic Wind Tunnel

### 1. What is the wind tunnel

A wind tunnel is a tool used in aerodynamic research to study the effects of air moving past solid objects. A wind tunnel consists of a tubular passage with the object under test mounted in the middle. Air is made to move past the object by a powerful fan system or other means. The test object often called a wind tunnel model, is instrumented with suitable sensors to measure aerodynamic forces, pressure distribution, or other aerodynamic-related characteristics. (Vertical Wind Tunnel, February, 1945)

### 1.1 Description of the Wind Tunnel

The airflow created by the fans that are entering the tunnel is itself highly turbulent due to the fan blade motion (when the fan is blowing air into the test section – when it is sucking air out of the test section downstream, the fan-blade turbulence is not a factor), and so is not directly useful for accurate measurements. The air moving through the tunnel needs to be relatively turbulence-free and laminar. To correct this problem, closely spaced vertical and horizontal air vanes are used to smooth out the turbulent airflow before reaching the subject of the testing. (Paul, 1993)

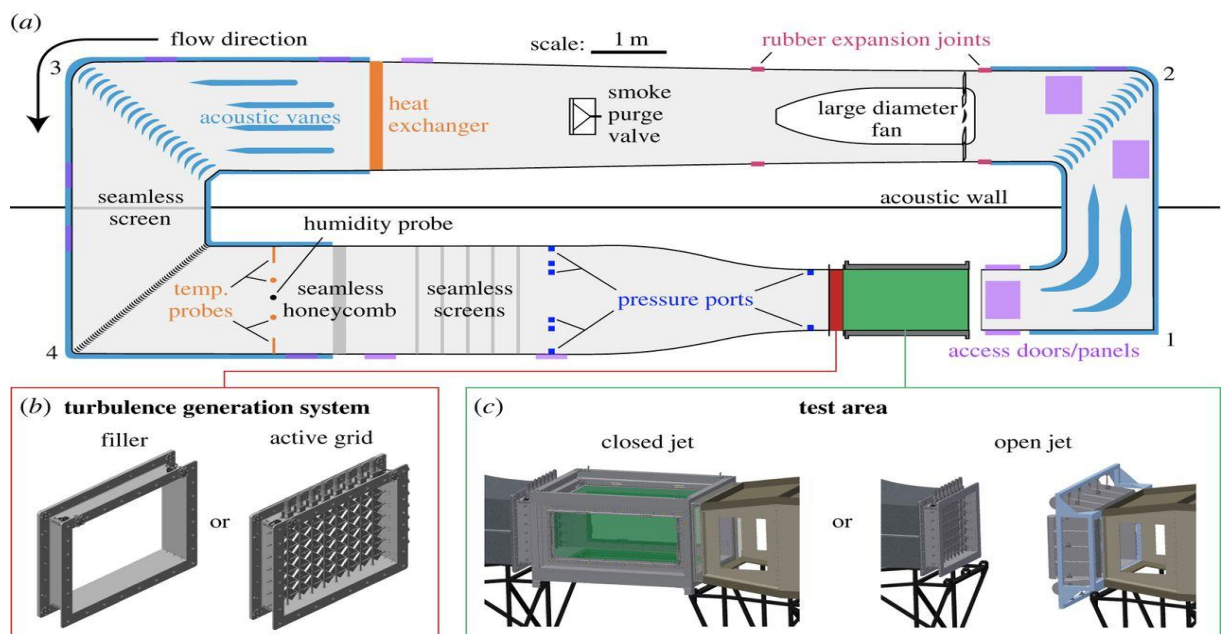


Figure 1 Open and closed types of wind tunnel

## CHAPTER 2-LITERATURE RESEARCH

### FUNDAMENTAL OF FLUID MECHANICS FOR LOW-SPEED WIND TUNNELS

#### 2.1 Boundary Layer

In wind tunnels, the Boundary Layer plays an essential role in experiments. It is for this reason that in this section a brief overview is given on that part of the subject matter. Two-dimensional boundary layers are recommended to decrease the disparity between theory and tests. Whenever any fluid flows over an object's surface the molecules of the last layer are likely to be attached to the surface of the object. Consequently, the velocity of this layer is identical with the object's velocity. In terms of the wind tunnel walls, this layer velocity will be zero; due to the wall shear stress, this specific condition is known as Slip Condition. The velocity of fluid varies from zero to maximum in upright layers. It is this type of layer, formed near the wall of the wind tunnel, known as Boundary Layer, where viscosity plays an important role. It leads to a laminar form at low ( $Re$ ), whereas the low converts to turbulent low as  $Re$  increase. According to the British physicist and engineer Osborne Reynolds, the general character of motion of fluids in contact with solid surfaces depends on the relation between a physical constant of fluid, and the product of the linear dimensions of space occupied by the fluid, and the velocity. If  $L$   $t$   $s$  complies with the length of the test section,  $U$   $t$   $s$  complies the velocity of air within the test section, then Reynolds number is shown by  $Re$ . Therefore one can rewrite all these parameters in the following (Kestin, 1962)

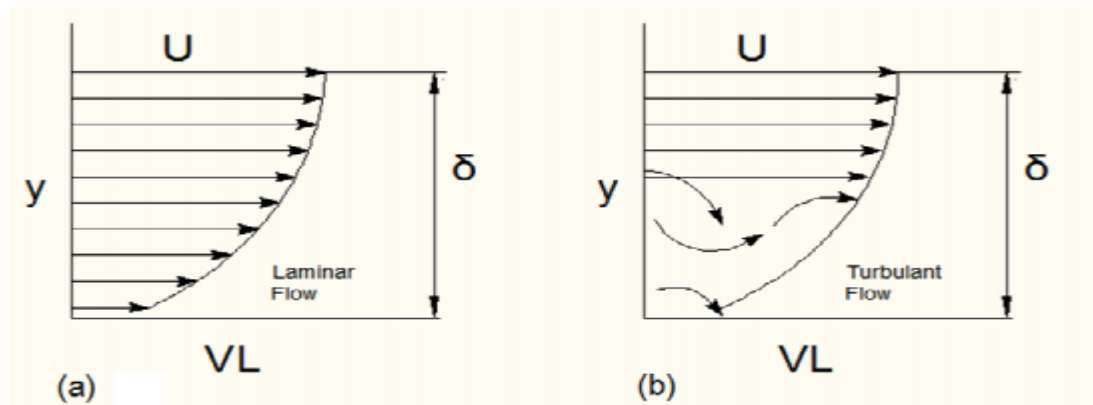


Figure 2 Boundary Layer representation with laminar flow and turbulent flow

Reynold Equation:

$$Re = \frac{v * D}{\nu} = Re = \frac{\text{inertial force}}{\text{viscous force}} = \frac{\text{fluid and flow properties}}{\text{fluid properties}} \quad (2.1)$$

Where  $\nu$  is kinetic viscosity and  $D$  is the hydraulic diameter

Figure 2. Shows the height of free stream velocity  $U$  from the wall of the wind tunnel.  $\Delta$  shows the Boundary layer thickness.  $U$  is the wall velocity. Figure 2. (a) Shows the laminar low in the boundary layer and figure 2. (b) Shows the turbulent low. There are many definitions for Laminar low. According to Smith fluid can low in one of two ways. One is in a smooth, layered fashion, in which the streamlines all remain in the same relative position with respect to each other. This type of flow is referred to as laminar flow. At high Reynold's numbers, the layer of air flow nearest to the wall surface acts as the wall surface. Due to many swirls being formed in this layer, all molecules become amalgamate, moving in an irregular fashion (Bauman) .

## 2.2 The Continuity Equation

The mathematical equation that represents the conservation of mass of moving fluid is known as the Continuity Equation. Suppose that fluid is in motion with the speed  $v$ , distance  $s$  moves as fluid in a time interval of  $\Delta t$  then  $s$  can be calculated as below:

$$s = v * \Delta t \quad (2.2)$$

Presumed that the fluid is in motion in a tube of a cross-sectional area of  $A$ , the volume  $V$  of the fluid can be express at a point as:

$$V = v * \Delta t * A \quad (2.3)$$

The mass flow rate of this fluid in the tube can be calculated by the following equation:

$$\frac{\Delta m}{\Delta t} = \rho * A * v \quad (2.4)$$

Where  $\rho$  is fluid density. If the mass of the fluid is constant between two points of the tube, this type of flow is called Steady Flow. As a result, the mass flow rate will be constant at both points. This can be expressed in the form of the following equation:

$$q_1 * A_1 * v_1 = q_2 * A_2 * v_2 \quad (2.5)$$

In the case that the fluid within the tube is incompressible and at low speed, its densities at both points of the tube should be the same. Thus the equation can be rewritten as:

$$A_1 * v_1 = A_2 * v_2 \quad (2.6)$$

### 2.3 Bernoulli Equation

Bernoulli's Equation basically represents the relation between velocity, density, and pressure. Since density is a constant, as explained in the previous section, the following equation expresses the relation of pressure and velocity between P2 and the conditions at P1 (Yunus A. Çengel, 2006):

$$P_1 + \frac{1}{2} * \frac{m}{v} * v^2 + \frac{m}{v} * g * h_1 = P_2 + \frac{1}{2} * \frac{m}{v} * v^2 + \frac{m}{v} * g * h_2 \quad (2.7)$$

In the following equation, presented by Nicholas in College Physics to understand more deeply the relation of pressure and velocity,  $\frac{m}{v}$  is the density of the fluid which can be written as  $\rho$ . Therefore one could rewrite it in the form below, known as Bernoulli's equation (Yunus A. Çengel, 2006);

$$P_1 + \frac{1}{2} * \rho * v_1^2 + \rho * g * h_1 = P_2 + \frac{1}{2} * \rho * v_2^2 + \rho * g * h_2 \quad (2.8)$$

$P_1, P_2$ - static pressure at point 1 and point 2

$v_1, v_2$ - flow speed at point 1 and point 2

$h_1, h_2$ - the height of two ends of the tube at point 1 and point 2

In the case that  $v = 0$  the pressure at two points is equal. Hence it only appears when the fluid is in motion. If the Bernoulli Equation is expressed in terms of the work-energy theorem, then the total mechanical energy of the fluid is conserved when moving from one place to the other. Still, a part of the energy is likely to be transferred from kinetic to potential or vice versa (Yunus A. Çengel, 2006).

The air flow through the wind tunnel will get pressure losses, which can be compensated by a raised pressure of the fans. As a result, the ratio between the lost pressure in a particular section and the dynamic pressure at the entrance of the wind tunnel can be written in the following form:

$$K1 = \frac{\Delta H}{\frac{1}{2}\rho_1 v_1^2} \quad (2.9)$$

Where K1 is the loss coefficient without dimension,  $\Delta H$  can be defined as head loss at the section of measurement of the loss coefficient.

### 2.3.1 Darcy-Welsbach

The Darcy–Welsbach equation is an empirical equation, which relates the head loss, or pressure loss, due to friction along a given length of pipe to the average velocity of the fluid flow for an incompressible fluid. The equation is named after Henry Darcy and Julius Welsbach.

The Darcy–Welsbach equation contains a dimensionless friction factor, known as the Darcy friction factor. This is also variously called the Darcy–Welsbach friction factor, friction factor, resistance coefficient, or flow coefficient.

$$\Delta H = \mu * \frac{L}{D} * \frac{v^2}{2g} \quad (2.10)$$

### 2.4 Reynold's and Mach number

The dimensionless Reynolds number plays a prominent role in foreseeing the patterns in a fluid's behavior. The Reynolds number, referred to as Re, is used to determine whether the fluid flow is laminar or turbulent. It is one of the main controlling parameters in all viscous flows where a numerical model is selected according to pre-calculated Reynolds number (Yunus A. Çengel, 2006).

Although the Reynolds number comprises both static and kinematic properties of fluids, it is specified as a flow property since dynamic conditions are investigated. Technically speaking, the Reynolds number is the ratio of the inertial forces and the viscous forces. In practice, the Reynolds number is used to predict if the flow will be laminar or turbulent (Yunus A. Çengel, 2006).

If the inertial forces, which resist a change in velocity of an object and are the cause of the fluid movement, are dominant, the flow is turbulent. Otherwise, if the viscous forces, defined as the resistance to flow, are dominant – the flow is laminar.

### 2.4.1 Fluid, Flow and Reynold's number

The applicability of the Reynolds number differs depending on the specifications of the fluid flow such as the variation of density (compressibility), a variation of viscosity (Non-Newtonian), being internal or external flow, etc. The critical Reynolds number is the expression of the value to specify transition among regimes which diversifies regarding the type of flow and geometry as well. Whilst the critical Reynolds number for turbulent flow in a pipe is 2000, the critical Reynolds number for turbulent flow over a flat plate, when the flow velocity is the free-stream velocity, is in a range from  $10^5$  to  $10^6$ .

The Reynolds number also predicts the viscous behavior of the flow in case fluids are Newtonian. Therefore, it is highly important to perceive the physical case to avoid inaccurate predictions. Transition regimes and internal as well as external flows with either low or high Reynolds number in use, are the basic fields to comprehensively investigate the Reynolds number. Newtonian fluids are fluids that have a constant viscosity. If the temperature stays the same, it does not matter how much stress is applied to a Newtonian fluid; it will always have the same viscosity. Examples include water, alcohol, and mineral oil (Yunus A. Çengel, 2006).

Internal flow;

Flow type	Reynold's number range
Laminar regime	Up to $Re=2300$
Transition Regime	$2300 < Re < 4000$
Turbulent Regime	$Re > 4000$

*Table 1 Flow Regimes*

Derivation;

The dimensionless Reynolds number predicts whether the fluid flow would be laminar or turbulent referring to several properties such as velocity, length, viscosity, and also type of flow. It is expressed as the ratio of inertial forces to viscous forces and can be explained in terms of units and parameters respectively, as equation 2.1:

### 2.4.2 Mach Number

The local speed of sound, and thereby the Mach number, depends on the condition of the surrounding medium, in particular, the temperature. The Mach number is primarily used to determine the approximation with which a flow can be treated as an incompressible flow. The medium can be a gas or a liquid. The boundary can be traveling in the medium, or it can be stationary while the medium flows along with it, or they can both be moving, with different velocities: what matters is their relative velocity with respect to each other. The boundary can be the boundary of an object immersed in the medium, or of a channel such as a nozzle, diffusers or wind tunnels channeling the medium. As the Mach number is defined as the ratio of two speeds, it is a dimensionless number. If  $Ma < 0.2-0.3$  and the flow is quasi-

steady and isothermal, compressibility effects will be small and simplified incompressible flow equations can be used (Graebel, 2001).

While the terms subsonic and supersonic, in the purest sense, refer to speeds below and above the local speed of sound respectively, aerodynamicists often use the same terms to talk about particular ranges of Mach values. This occurs because of the presence of a transonic regime around  $Ma = 1$  where approximations of the Navier-Stokes equations used for subsonic design no longer apply; the simplest explanation is that the flow around an airframe locally begins to exceed  $Ma = 1$  even though the freestream Mach number is below this value.

Meanwhile, the supersonic regime is usually used to talk about the set of Mach numbers for which linearized theory may be used, where for example the (air) flow is not chemically reacting, and where heat-transfer between air and vehicle may be reasonably neglected in calculations (Hall, Mach Number).

In figure 2.1, the regimes or ranges of Mach values are referred to, and not the pure meanings of the words subsonic and supersonic.

Generally, NASA defines high hypersonic as any Mach number from 10 to 25, and re-entry speeds as anything greater than Mach 25. Aircraft operating in this regime include the Space Shuttle and various space planes in development.

### Mach Number Flow Regimes

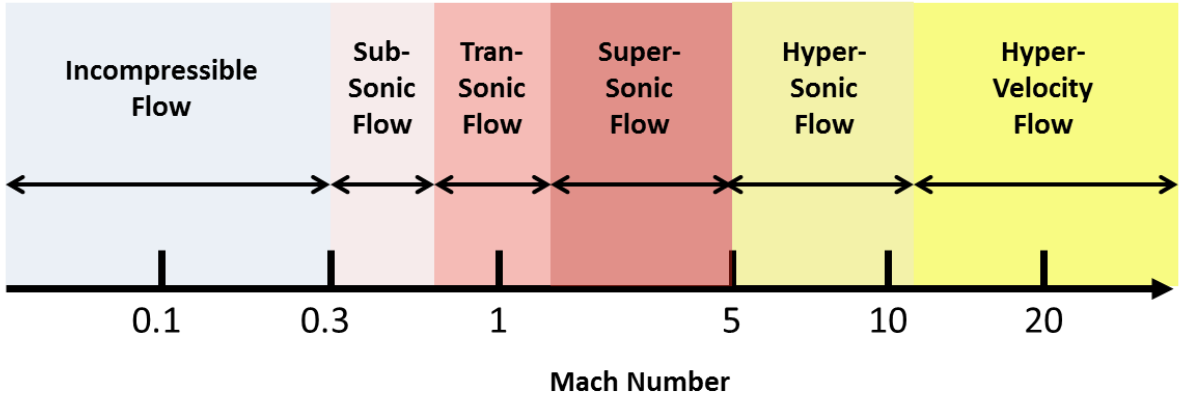


Figure 2.1 Mach number regimes

Formulation of Mach number;

$$Ma = \frac{v}{c} \tag{2.11}$$

$$c = \sqrt{k * R * T} \tag{2.12}$$

The speed of sound is the distance traveled per unit time by a sound wave as it propagates through an elastic medium.

k: specific heat ratio of air, R: gas constant, T: temperature of the air, c: speed of sound

The subsonic speed range is that range of speeds within all of the airflow over an aircraft is less than Mach 1. The critical Mach number ( $M_{crit}$ ) is the lowest free stream Mach number at which airflow over any part of the aircraft first reaches Mach 1. So the subsonic speed range includes all speeds that are less than  $M_{crit}$ .

$$Ma_{*} = Ma \sqrt{\frac{k+1}{2+(k+1)Ma^2}} \quad (2.13)$$

Mach formulation (2.14) is represented for the critical area of nozzle and calculated by local Mach number

### 2.4.3 Description of specific heat ratio of air

In thermal physics and thermodynamics, the heat capacity ratio or adiabatic index or ratio of specific heats or Poisson constant is the ratio of the heat capacity at constant pressure ( $C_P$ ) to heat capacity at constant volume ( $C_V$ ). It is sometimes also known as the *isentropic expansion factor* and is denoted by  $\gamma$  (gamma) for an ideal gas or  $\kappa$  (kappa), the isentropic exponent for a real gas. The symbol gamma is used by aerospace and chemical engineers.

$$k = \frac{C_p}{C_v} \quad (2.14)$$

Where  $C_p$  is the heat capacity, and  $c$  the specific heat capacity (heat capacity per unit mass) of a gas. The suffixes  $P$  and  $V$  refer to constant pressure and constant volume conditions respectively.

The heat capacity ratio is important for its applications in thermodynamically reversible processes, especially involving ideal gases; the speed of sound depends on that factor.

To understand this relation, consider the following thought experiment. A closed pneumatic cylinder contains air. The piston is locked. The pressure inside is equal to atmospheric pressure. This cylinder is heated to a certain target temperature. Since the piston cannot move, the volume is constant. The temperature and pressure will rise. When the target temperature is reached, the heating is stopped. The amount of energy added equals  $C_v \Delta T$ , with  $\Delta T$  representing the change in temperature. The piston is now freed and moves outwards, stopping as the pressure inside the chamber reaches atmospheric pressure. We assume the expansion occurs without the exchange of heat (adiabatic expansion). Doing this work, the air inside the cylinder will cool to below the target temperature. To return to the target temperature (still with a free piston), the air must be heated, but is no longer under constant volume, since the piston is free to move as the gas is reheated. This extra heat amounts to about 40% more than the previous amount added.



In this example, the amount of heat added with a locked piston is proportional to  $C_V$ , whereas the total amount of heat added is proportional to  $C_P$ . Therefore, the heat capacity ratio in this example is 1.4.

Ideal gas relation;

For an ideal gas, the heat capacity is constant with temperature. Accordingly, we can express the enthalpy as  $H = C_P T$  and the internal energy as  $U = C_V T$ . Thus, it can also be said that the heat capacity ratio is the ratio between the enthalpy to the internal energy:

$$k = \frac{H}{U} \quad (2.15)$$

Furthermore, the heat capacities can be expressed in terms of heat capacity ratio ( $\gamma$ ) and the gas constant ( $R$ ):

$$C_P = \frac{k * n * R}{k - 1} \quad C_V = \frac{n * R}{k - 1} \quad (2.16)$$

Where  $n$  is the amount of substance in moles.

Mayer's relation allows to deduce the value of  $C_V$  from the more commonly tabulated value of  $C_P$ :

$$C_V = C_P - n * R \quad (2.17)$$

Relation with degrees of freedom;

The heat capacity ratio ( $\gamma$ ) for an ideal gas can be related to the degrees of freedom ( $f$ ) of a molecule by;

$$k = 1 + \frac{2}{f} \quad f = \frac{2}{k - 1} \quad (2.18)$$

Thus we observe that for a monatomic gas, with 3 degrees of freedom:

$$k = \frac{5}{3} = 1.66$$

While for a diatomic gas, with 5 degrees of freedom (at room temperature: 3 translational and 2 rotational degrees of freedom; the vibrational degree of freedom is not involved, except at high temperatures)

$$k = \frac{7}{5} = 1.4$$

For example, the terrestrial air is primarily made up of diatomic gases (around 78% nitrogen (N<sub>2</sub>) and 21% oxygen (O<sub>2</sub>)), and at standard conditions, it can be considered to be an ideal gas. The above value of 1.4 is highly consistent with the measured adiabatic indices for dry air within a temperature range of 0–200 °C, exhibiting a deviation of only 0.2%

## CHAPTER 3

### DESIGNING THE LOW-SPEED WIND TUNNEL

#### 3.1 Wind Tunnel classification

Wind tunnels can be classified in two categories on the basis of geometry, the first being Open Loop Wind Tunnels and the second Closed Loop Wind Tunnels. Further predetermined requirements in terms of performance and dimensions of the Wind Tunnel, as well as technical means, are listed in the table below:

Type	Subsonic Model
The maximum speed of exit of the nozzle	50 m/s
Minimum speed	2 m/s
Visualization	With smoke

*Table 2 initial data*

##### 3.1.1 Closed Loop Wind tunnel

In contrast to the previously depicted type, this category of wind tunnels is characterized by loop feedback to its contraction. Besides the sections of contraction, test section, diffuser, and fan it consists also of the additional sections of turning vanes and the loop. Definite advantages of a Closed Loop Wind Tunnel are high-quality flow, as well as a decrease of pressure loss. The category can be divided into the following two subcategories (Hall, NASA, 2015):

The Open Test Section in which air is blown from the contraction cone to an open space between the contraction area and the diffuser. The test model is usually placed in this space. This type of test section creates much higher pressure loss.

The Closed Test Section in which air is blown from the contraction cone to a closed wall test section. The test model is usually located in this closed wall section. The walls of the test section cause Wall friction.

### Advantages of closed type;

1. Superior flow quality in the test section. Flow turning vanes in the corner and flow straighteners near the test section insure relatively uniform flow in the test section.
2. Low operating costs. Once the air is circulating in the tunnel, the fan and motor only need to overcome losses along the wall and through the turning vanes. The fan does not have to constantly accelerate the air.
3. Quiet operation relative to an open return tunnel.

### Disadvantages of closed type

1. Higher construction cost because of the added vanes and ducting.
2. Inferior design for propulsion and smoke visualization. The tunnel must be designed to purge exhaust products that accumulate in the tunnel.
3. Hotter running conditions than an open return tunnel. The tunnel may have to employ heat exchangers or active cooling.

## 3.2 Theory of Specific design

We have our investigation sections where are the test section and the nozzle section. According to our aim, we should model our system within specific parameters which means design for ‘‘Incompressible De-Laval nozzle’’ and ‘‘rectangular pipe line test section’’. The optimal design must have actualized the conditions to reach a turbulent flow regime and subsonic type controlled by Mach number.

### 3.2.1 Subsonic De-Laval nozzle

A nozzle is an extremely efficient device for converting thermal energy to kinetic energy. Nozzles come up in a vast range of applications. Obvious ones are the thrust nozzles of rocket and jet engines. Converging-diverging ducts also come up in aircraft engine inlets, wind tunnels and in all sorts of piping systems designed to control gas flow. The flows associated with volcanic and geyser eruptions are influenced by converging-diverging nozzle geometries that arise naturally in geological formations (Carswell, 2007).

### 3.2.1.1 Theoretical description of De-Laval nozzle

De-Laval nozzle model definable as a hyperbola plane curve which can be represented by one of the equations;

$$\frac{x^2}{a^2} - \frac{y^2}{b^2} = \pm 1 \quad (3.1)$$

Equations are called the canonical equations of the hyperbola.

In this system, the coordinate axes are axes of symmetry, and so if a point  $(x,y)$  belongs to the hyperbola then the points  $(-x,y)$ ,  $(x,-y)$  and  $(-x,-y)$  also belong to the hyperbola (Konev, 2001-2009).

The intersection points of the hyperbola with the axis of symmetry are called the vertices of the hyperbola. Any hyperbola has two vertices.

If  $a = b$  then the hyperbola is called an equilateral hyperbola.

The equation based on;

$$\frac{(x-x_0)^2}{a^2} - \frac{(y-y_0)^2}{b^2} = \pm 1 \quad (3.2)$$

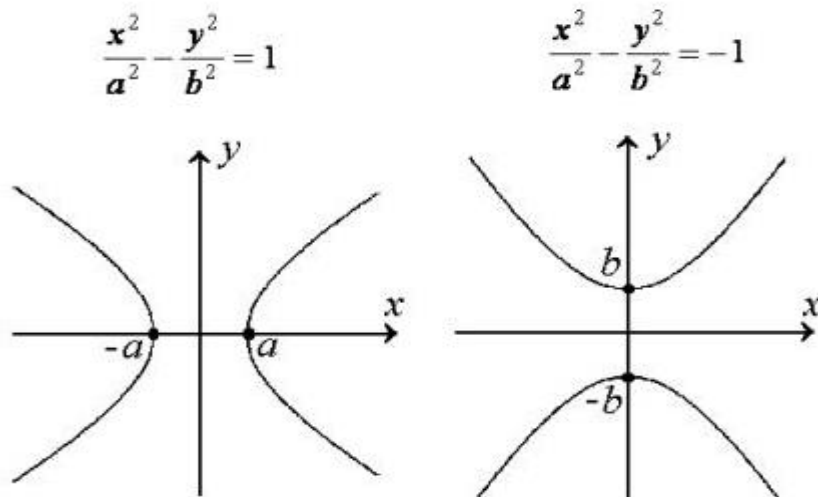


Figure 3 Illustration of hyperbolic equations (right side is our nozzle type) (Konev, 2001-2009)

After considering the shape of De-Laval nozzle we describe of inlet section and critical section diameter. The attention is on half of De-Laval nozzle which means convergence type nozzle.

The convergence type of nozzle has an outlet section where the critical section is approved as Mach number is equal 1.

When we follow theoretical terms of incompressible and compressible fluid flow that shows some equations based on air flow in nozzle systems (Cantwell, 2015).

Area averaged equations of motion (Cantwell, 2015);

$$\begin{aligned}
 d(q * U) &= \frac{\Delta m}{A} - q * U * \frac{dA}{A} \\
 d(P - t_{xx}) + q * U dU &= -\frac{1}{2} * q * U^2 \left( \frac{4Cf dx}{D} \right) + \frac{(U_{xx} - U) \Delta m}{A} - \frac{\Delta F_x}{A} \\
 d \left( ht - \frac{t_{xx}}{q} + \frac{Q_{xx}}{q * U} \right) &= \Delta q w - \Delta w + (htm - \left( ht - \frac{t_{xx}}{q} + \frac{Q_{xx}}{q * U} \right)) \frac{\Delta m}{q * U * A}
 \end{aligned} \tag{3.3}$$

Assume the only effect on the flow is stream wise area change so that (Cantwell, 2015);

$$\Delta m = Cf = \Delta F_x = \Delta q = \Delta w = 0. \tag{3.4}$$

Also assume that stream wise normal stresses and heat fluxes  $t_{xx}$ ,  $Q_{xx}$  are small enough to be neglected. With these assumptions the governing equations (3.3) together with the perfect gas law reduce to (Cantwell, 2015);

$$\begin{aligned}
 d(q * U * A) &= 0 \\
 dP + q U dU &= 0 \\
 Cp dT + U dU &= 0 \\
 P &= q * R * T
 \end{aligned} \tag{3.5}$$

Introduce to Mach number (Cantwell, 2015);

$$U^2 = k * R * T * Ma^2 \tag{3.6}$$

Each of the equations in (3.5) can be expressed in fractional differential form;

$$\begin{aligned}
\frac{dq}{q} + \frac{dU^2}{2U^2} + \frac{dA}{A} &= 0 \\
\frac{dp}{p} + \frac{kMa^2}{2} * \frac{dU^2}{U^2} &= 0 \\
\frac{dT}{T} + \frac{(k-1)Ma^2}{2} * \frac{dU^2}{U^2} &= 0 \\
\frac{dP}{P} &= \frac{dq}{q} + \frac{dT}{T}
\end{aligned} \tag{3.7}$$

Equation (3.6) can also be written in fractional differential form;

$$\frac{dU^2}{U^2} = \frac{dT}{T} + \frac{dMa^2}{Ma^2} \tag{3.8}$$

Use the equations for mass, momentum, and energy to replace the terms in the equation of state;

$$-\frac{kMa^2}{2} * \frac{dU^2}{U^2} = -\frac{dU^2}{2U^2} - \frac{dA}{A} - \frac{(k-1)Ma^2}{2} * \frac{dU^2}{U^2} \tag{3.9}$$

Solve for  $\frac{dU^2}{U^2}$ ;

$$\frac{dU^2}{U^2} = \left( \frac{2}{Ma^2-1} \right) \frac{dA}{A} \tag{3.10}$$

Equation (3.10) shows the effect of stream wise area change on the speed of the flow. If the Mach number is less than one then increasing area leads to a decrease in the velocity. But if the Mach number is greater than one then increasing area leads to an increase in flow speed. Use (3.10) to replace  $\frac{dU^2}{U^2}$  in each of the relations in (3.7);

$$\begin{aligned}
\frac{dq}{q} &= -\left( \frac{Ma^2}{Ma^2-1} \right) \frac{dA}{A} \\
\frac{dP}{P} &= -\left( \frac{kMa^2}{Ma^2-1} \right) \frac{dA}{A}
\end{aligned} \tag{3.11}$$

$$\frac{dT}{T} = -\left(\frac{(k-1)Ma^2}{Ma^2-1}\right) \frac{dA}{A}$$

Equations (3.11) describe the effects of area change on the thermodynamic state of the flow. Now use (3.10) and the temperature equation in (3.8);

$$\left(\frac{2}{Ma^2-1}\right) \frac{dA}{A} = -\frac{(k-1)Ma^2}{Ma^2-1} * \frac{dA}{A} + \frac{dMa^2}{Ma^2} \quad (3.12)$$

The effect of area change on the Mach number is;

$$\frac{dA}{A} = \frac{Ma^2-1}{2(1+\left(\frac{k-1}{2}\right)Ma^2)} * \frac{dMa^2}{Ma^2} \quad (3.13)$$

Equation (3.13) is different from (3.10) and (3.11) in that it can be integrated from an initial to a final state. Integrate (3.13) from an initial Mach number Ma to one;

$$\int_{Ma^2}^1 \frac{Ma^2-1}{2(1+\left(\frac{k-1}{2}\right)Ma^2)} \frac{dMa^2}{Ma^2} = \int_A^{A^*} \frac{dA}{A} \quad (3.14)$$

The Result is;

$$\ln\left(\frac{A^*}{A}\right) = \left\{ -\ln Ma + \ln\left(2\left(1 + \left(\frac{k-1}{2}\right) * Ma^2\right)^{\frac{k+1}{2*(k-1)}}\right) \right\} \quad (3.15)$$

The result is the all-important area-Mach number equation;

$$f(Ma) = \frac{A^*}{A} = \left(\frac{k+1}{2}\right)^{\frac{k+1}{2(k-1)}} * \frac{Ma}{\left(1+\left(\frac{k-1}{2}\right)Ma^2\right)^{\frac{k+1}{2(k-1)}}} \quad (3.16)$$

In (3.16) we referenced the integration process to Ma = 1. The area A\* is a reference area at some point in the channel where Ma = 1 although such a point need not actually be present in

a given problem. The area-Mach-number function is plotted figure 3.1 for three values of  $k$ . Note that for smaller values of it takes an extremely large area ratio to generate high Mach number flow. A value of  $k = 1.2$  would be typical of the very high-temperature mixture of gases in a rocket exhaust. Conversely, if we want to produce a high Mach number flow in a reasonable size nozzle, say for a wind tunnel study, an effective method is to select a monatomic gas such as Helium which has  $k = 1.66$ . A particularly interesting feature of (3.16) is the insensitivity of  $f(M)$  to  $k$  for subsonic flow. But in our system, we use air and  $k=1.4$ .

Mass Conservation

The result (3.16) can also be derived simply by equating mass flows at any two points in the channel and using the mass flow relation (Cantwell, 2015).

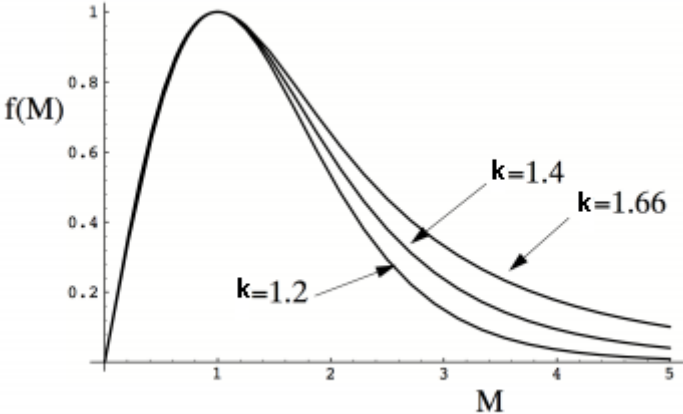


Figure 3.1 Area-Mach number function (Cantwell, 2015)

Mass flow rate;

$$\dot{m} = \rho * v * A \tag{3.17}$$



This can be expressed as;

$$\dot{m} = q * v * A = \frac{P}{R*T} (k * R * T)^{\frac{1}{2}} * Ma * A \quad (3.18)$$

Thus;

$$\begin{aligned} \frac{T_0}{T} &= 1 + \frac{k-1}{2} * Ma^2 \\ \frac{P_0}{P} &= \left(1 + \frac{k-1}{2} * Ma^2\right)^{\frac{k}{k-1}} \\ \frac{q_0}{q} &= \left(1 + \left(\frac{k-1}{2}\right) * Ma^2\right)^{\frac{1}{k-1}} \\ \frac{A_0}{A^*} &= \frac{1}{M} \left(\left(\frac{2}{k+1}\right) \left(1 + \left(\frac{k-1}{2}\right) * Ma^2\right)\right)^{\frac{k+1}{2(k-1)}} \\ \dot{m} &= \frac{A * Ma * P_0 \sqrt{k/(R*T_0)}}{\left[\frac{1+(k-1)Ma^2}{2}\right]^{\frac{(k+1)}{2*(k-1)}}} \end{aligned} \quad (3.19)$$

The isentropic assumption works quite well for nozzles that are encountered in most applications. But if the plenum falls below a few centimeters in size with a nozzle diameter less than a few millimeters then a fully viscous, non-isentropic treatment of the flow is required. Accurate nozzle design, regardless of size, virtually always requires that the boundary layer on the wall of the plenum and nozzle is taken into account. If the ambient pressure equals the reservoir pressure there is, of course, no flow. If  $P_{\text{ambient}}$  is slightly below  $P_t$  then there is a low-speed, subsonic, approximately isentropic flow from the plenum to the nozzle. If  $P_t/P_{\text{ambient}}$  is less than a certain critical value then the condition that determines the speed of the flow at the exit is that the exit static pressure is very nearly equal to the ambient pressure (Cantwell, 2015).

The reason this condition applies is that large pressure differences cannot occur over small distances in subsonic flow. Any such difference that might arise, say between the nozzle exit and a point slightly outside of and above the exit, will be immediately smoothed out by a readjustment of the whole flow. Some sort of shock or expansion is required to maintain a pressure discontinuity and this can only occur in supersonic flow. Slight differences in pressure are present due to the mixing zone that exists outside the nozzle but in subsonic flow, these differences are very small compared to the ambient pressure. Since the flow up to the exit is approximately isentropic the stagnation pressure  $P_t$  is approximately constant from the reservoir to the nozzle exit

## Exit Velocity of Nozzle

The Energy equation is a statement of the principle of the conservation of energy. For isentropic flow between any two points and it's given by

$$h_1 - h_2 = \frac{1}{2}(v_2^2 - v_1^2) = Cp(T_1 - T_2) \quad (3.19.1)$$

Where h represents enthalpy of the fluid (which can be considered the energy available for heat transfer), v is the flow velocity, Cp is the effective heat capacity of the fluid, and T is the fluid temperature. This equation provides valuable insight into how a nozzle works. Looking at the first two terms shows that the change (decrease) in enthalpy is equal to the change (increase) in the kinetic energy. In other words, the heat of the fluid is being used to accelerate the flow to a greater velocity. The third term represents the resulting change (decrease) in temperature of the flow. The heat capacity may be approximated to be constant and is a property determined by the composition of the combustion products (Borgnakke, 2009).

It's apparent, then, that the properties of a fluid are a function of the flow velocity. In describing the state of a fluid at any point along with its flow, it is convenient to consider the stagnation state as a reference state. The stagnation properties may be considered as the properties that would result if the fluid were (isentropically) decelerated to zero velocity (Borgnakke, 2009).

$$T_0 = T + \frac{v^2}{2 \cdot Cp} \quad (3.19.2)$$

For an isentropic flow process, the following important relationship between stagnation properties for Temperature, Pressure, and Fluid Density hold;

$$\frac{T_0}{T} = \left(\frac{P_0}{P}\right)^{\frac{k-1}{k}} = \left(\frac{\rho_0}{\rho}\right)^{k-1} \quad (3.19.3)$$

Where k is the all-important ratio of specific heats, also referred to as the isentropic exponent, defined as;

$$k = \frac{Cp}{Cv} = \frac{Cp}{Cp - R} \quad (3.19.4)$$

Both Cp and R (specific gas constant) are properties determined by the composition of the combustion products, where  $R = R'/M$ , where R' is universal gas constant, and M is the effective molecular weight of the combustion products. If the combustion products contain an appreciable percentage of condensed phase particles, the value of the effective molecular weight.

From equations (3.19.1), (3.19.2), (3.19.3) Mach number may write;

$$\frac{T_0}{T} = 1 + \frac{k-1}{2} * Ma^2 \quad (3.19.5)$$

It can be shown from the first and second laws of thermodynamics, for any isentropic process;

$$\frac{P}{q^k} = constant \quad (3.19.6)$$

From equation (3.19.5) and (3.19.6) from the equation of state for an ideal gas,  $P = q * R * T$ , the relationship between stagnation pressure, density and Mach number may be expressed as given;

$$\frac{P_0}{P} = \left(1 + \frac{k-1}{2} * Ma^2\right)^{\frac{k}{k-1}} \quad (3.19.7)$$

$$\frac{q_0}{q} = \left(1 + \frac{k-1}{2} * Ma^2\right)^{\frac{1}{k-1}} \quad (3.19.8)$$

Another important stagnation property is the stagnation enthalpy;

$$h_0 = h + \frac{v^2}{2} \quad (3.19.9)$$

From equations (3.19.9) and (2.5);

$$v_{exit} = \sqrt{2 * (h_x - h_{exit}) + (v_x)^2} \quad (3.19.10)$$

Where subscripts e and x signify exit and any point x along the nozzle axis, respectively. This equation can then be put into the far more useful form with the aid of the energy equation and the definition of k.

$$v_{exit} = \sqrt{\frac{T^*R}{Ma} * \frac{2k}{k-1} * \left[1 - \left(\frac{P^*}{P_0}\right)^{\frac{k-1}{k}}\right]} \quad (3.19.11)$$

### 3.2.2 Geometry description of the test section

The test section is the part of the wind tunnel in which the model is placed. For low-speed tunnel operation, the test section has the smallest cross-sectional area and the highest velocity within the tunnel. Leaving the test section, the air enters the diffuser where it is expanded and slowed before returning to the fan. Again, the diffuser is employed to minimize losses in the

tunnel. For this closed circuit wind tunnel, there are two more corners with turning vanes before the air is brought back to the fan (Ge, 2015).

Wind tunnels are designed for a specific purpose and speed range and there is a wide variety of wind tunnel types and model instrumentation. The model to be tested in the wind tunnel is placed in the test section of the tunnel. The speed in the test section is determined by the design of the tunnel. The choice of speed range affects the design of the wind tunnel due to compressibility effects.

For subsonic flows, the air density remains nearly constant and decreasing the cross-sectional area causes the flow to increase velocity and decrease pressure. Similarly, increasing the area causes the velocity to decrease and the pressure to increase. We want the highest possible velocity in the test section. For a subsonic wind tunnel, the test section is placed at the end of the contraction section and upstream of the diffuser. From a knowledge of the conservation of mass for subsonic flows, we can design the test section to produce the desired velocity or Mach number since the velocity is a function of the cross-sectional area (Ge, 2015).

For subsonic flows, the air density changes very small in the tunnel because of compressibility. In fact, the density changes faster than the velocity by a factor of the square of the Mach number. In subsonic flow, decreasing the cross-sectional area causes the flow to increase in velocity and decrease pressure. Similarly, increasing the area causes the velocity to decrease and the pressure to increase. This change in properties is exactly the opposite of the change that occurs sub-sonically. In addition, compressible flows experience mass flow choking. As a subsonic flow is contracted, the velocity and Mach number increase. When the velocity reaches the speed of sound ( $M = 1$ ), the flow chokes and the Mach number cannot be increased beyond  $M = 1$ . We want the highest possible velocity in the test section of the wind tunnel. For a subsonic wind tunnel, we contract the flow until it chokes in the throat of a nozzle. We then diffuser the flow which increases the speed sub-sonically. The test section of the subsonic tunnel is placed at the end of the diffuser. From a consideration of conservation of mass for compressible flow, we can design the test section to produce a desired velocity or Mach based on the area in the test section. (Ge, 2015).

We have a test section which is given to use and measurements are as;

Length	10m
height	4,356m
width	4.356m
Support of test section	1,178m
The thickness of the wall of the test section	0,4 m

*Table 3 Given Measurements of the test section*

## CHAPTER 4-PRACTICAL PART

### ANALYTICAL CALCULATIONS

#### 4.1 De-Laval nozzle measurements calculation

We start to calculate with the shape of De-Laval nozzle and design according to our measurements.

According to the equation (3.2);

T*(exit temperature)	20	Celsius
P0(initial pressure)	101	kpa
Ve (exit velocity)	50	m/s
R(air gas constant)	287,058	kJ/kg*K
C(speed of sound)	343	m/s
k (specific heat ratio)	1.4	

*Table 4 given and considered Values of the system*

Mach number of the system;

(2.13) and (2.14) equations are used to calculate Mach number to reach subsonic values within nozzle and test section

$$C = \sqrt{1.4 * 287.058 * (273,15 + 20)} = 343 \text{ m/s}$$

$$Ma = \frac{50}{343} = 0.145$$

Inlet and outlet area ratio;

According to (3.19) A/A\* equation which depends on the specific heat ratio and Mach number and we already have both of values.

$$\begin{aligned} \frac{A_0}{A^*} &= \frac{1}{M} \left( \left( \frac{2}{k+1} \right) \left( 1 + \left( \frac{k-1}{2} \right) * Ma^2 \right) \right)^{\frac{k+1}{2(k-1)}} \\ &= \frac{1}{0.145} \left( \left( \frac{2}{2+1.4} \right) \left( 1 + \left( \frac{1.4-1}{2} \right) * 0.145^2 \right) \right)^{\frac{1.4+1}{2(1.4-1)}} = 3.9129 \end{aligned}$$

$$\frac{A_0}{A^*} = \frac{\pi(r_0)^2}{\pi(r_1)^2} = 3.9129$$

$$\sqrt{\frac{r_0}{r_1}} = \sqrt{3.9129} = 1.9781$$

$$\frac{r_0}{r_1} = 1.9781$$

We desire to design our nozzle for that ratio and considered inlet and outlet as cylindrical shape  
 $D_0=1.9781*2=3.95$  m and  $D^*=1*2=2$  m

Hyperbola definition;

The hyperbola can also be defined as a set of points in the coordinate plane. A hyperbola is the set of all points  $(x,y)$  in a plane such that the difference of the distances between  $(x,y)$  and the foci is a positive constant.

Notice that the definition of a hyperbola is very similar to that of an ellipse. The distinction is that the hyperbola is defined in terms of the difference of two distances, whereas the ellipse is defined in terms of the sum of two distances.

As with the ellipse, every hyperbola has two axes of symmetry. The transverse axis is a line segment that passes through the center of the hyperbola and has vertices as its endpoints. The foci lie on the line that contains the transverse axis. The conjugate axis is perpendicular to the transverse axis and has the co-vertices as its endpoints. The center of a hyperbola is the midpoint of both the transverse and conjugate axes, where they intersect. Every hyperbola also has two asymptotes that pass through its center (Miller, 2017).

As a hyperbola recedes from the center, its branches approach these asymptotes. The central rectangle of the hyperbola is centered at the origin with sides that pass through each vertex and co-vertex; it is a useful tool for graphing the hyperbola and its asymptotes. To sketch the asymptotes of the hyperbola, simply sketch and extend the diagonals of the central rectangle (Miller, 2017)

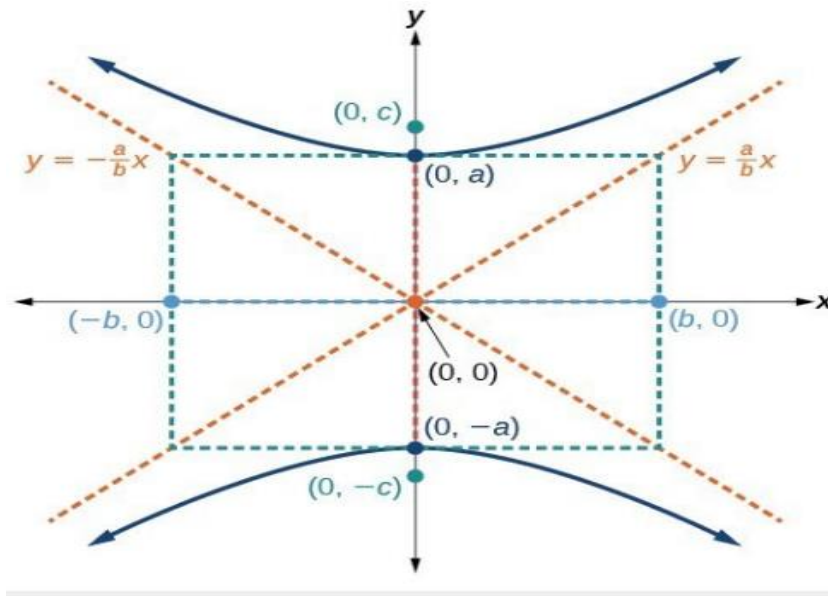


Figure 4 Illustration of hyperbole equation (Miller, 2017)

Identify the horizontal and foci of the hyperbola with equation Radius ratio is directly proportionate to a and b values on the hyperbola equation;

$$a = 1,97 \text{ and } b = 1$$

Thus equation (3.2);

$$\frac{y^2}{1,97^2} - \frac{x^2}{1^2} = 1$$

Correspondingly and due to (3.2) equation;

$$y^2 - 3,9x^2 = 3,9$$

Our r0 and r\* values 3, 95 and 2 respectively, therefore;

*According to (3.2) equation  $x = 0$   $y = 1,978$  it represents  $r^*$*

For that;

*In order to reach  $y = 3,956$  and  $x = 1,733$*

X represents the length of nozzle and Y represents inlet and outlet diameter.

So that;

We have already our design measurements as semi-diameter to produce shape and system.

r*	1	meter
r0	1,9781	meter
Length of nozzle	1,73	meter

Table 4.1 Calculated measurements of De-Laval nozzle

#### 4.1.1 Temperature, Pressure, Density ratio and Exit, Inlet velocity in De-Laval nozzle

Temperature ratio declaring; temperature ratio depends on k specific heat ratio and Mach number, we develop relations between the static properties and stagnation properties of an ideal gas in terms of the specific heat ratio k and the Mach number Ma. We assume the flow is isentropic and the gas has constant specific heats. The temperature T of an ideal gas anywhere in the flow is related to the stagnation temperature T0.

According to equation (3.19);

$$\frac{T_0}{T} = 1 + \frac{k-1}{2} * Ma^2$$

$$\frac{T_0}{T} = 1 + \frac{(1.4)-1}{2} * (0.145)^2$$

$$\frac{T_0}{T} = 1.004205$$

Pressure Ratio declaring;

The ratio of the stagnation to static pressure is obtained by substituting;

$$\frac{P_0}{P} = \left(1 + \frac{k-1}{2} * Ma^2\right)^{\frac{k}{k-1}}$$

$$\frac{P_0}{P} = \left(1 + \frac{1.4-1}{2} * (0.145)^2\right)^{\frac{1.4}{1.4-1}}$$

$$\frac{P_0}{P} = 1.01479$$



Density Ratio Declaring;

The ratio of the stagnation to static density is obtained by substituting

$$\frac{q_0}{q} = \left(1 + \left(\frac{k-1}{2}\right) * Ma^2\right)^{\frac{1}{k-1}}$$

$$\frac{q_0}{q} = \left(1 + \left(\frac{1.4-1}{2}\right) * (0.145)^2\right)^{\frac{1}{1.4-1}}$$

$$\frac{q_0}{q} = 1.01054$$

Numerical values of  $T/T_0$ ,  $P/P_0$ , and  $q/q_0$  are listed versus the Mach number In The Gas Dynamic Table for k 1.4, which are very useful for practical compressible flow calculations involving air.

Calculation of exit velocity of a nozzle according to equation (3.19.12)

$$v_{exit} = \sqrt{\frac{T^*R}{Ma}} * \frac{2k}{k-1} * \left[1 - \left(\frac{P^*}{P_0}\right)^{\frac{k-1}{k}}\right]$$

$$v_{exit} = \sqrt{\frac{293,15*287}{0.145}} * \frac{2*1.4}{1.4-1} * \left[1 - (0.9854)^{\frac{1.4-1}{1.4}}\right]$$

$$v_{exit} = 26.66 \text{ m/s}$$

Calculation of inlet velocity of the nozzle by continuity equation (3.19.10);

$$A_1 * v_1 = A_2 * v_2$$

$$3.9129 * v_1 = 1 * 26.66$$

$$v_1 = v_{inlet \text{ of nozzle}} = 6.9 \text{ m/s}$$

Calculation of velocity of system inlet by continuity equation (3.19.10);

$$A_1 * v_1 = A_{system \text{ inlet}} * v_{system \text{ inlet}}$$

$$(3.14 * 3.9129) * 6.9 = 15.06 * v_{system \text{ inlet}}$$

$$v_{system \text{ inlet}} = 5.5 \text{ m/s}$$

#### 4.1.2 Demonstration of analytical calculations by The Gas Dynamic Table;

### GAS DYNAMIC TABLE Genick Bar-Meir

Gas Dynamic Calculator, (Potto–GDC) was created to generate various tables for the exercises. This calculator was given to several individuals and they found Potto–GDC to be very useful. So, I decided to include Potto–GDC to the thesis. This table (4.2 and 4.3) calls as oblique shock table which is the shock occurs (given for  $k=1.4$ ) in reality in situations where the shock has three–dimensional effects. The three–dimensional effects of the shock make it appear as a curved plane. However, one–dimensional shock can be considered a representation for a chosen arbitrary accuracy with a specific small area. In such a case, the change of the orientation makes the shock considerations two–dimensional. The normal shock analysis dictates that after the shock, the flow is always Subsonic. The total flow after the oblique shock can also be supersonic, which depends on the boundary layer and the deflection angle. The velocity has two components (with respect to the shock plane/surface). Only the oblique shock's normal component undergoes the "shock." The tangent component does not change because it does not "move" across the shock line.

#### 1.1.3 Isentropic Flow for $k = 1.4$

Table 1.3: Isentropic Flow for  $k=1.4$

M	$\frac{T}{T_0}$	$\frac{\rho}{\rho_0}$	$\frac{A}{A^*}$	$\frac{P}{P_0}$	$\frac{A \times P}{A^* \times P_0}$	$\frac{F}{F^*}$
0.0	1.00000	1.00000	5.8E+5	1.00000	5.8E+5	2.4E+5
0.05	0.99950	0.99875	11.59	0.99825	11.57	4.838
0.1	0.99800	0.99502	5.822	0.99303	5.781	2.443
0.20	0.99206	0.98028	2.964	0.97250	2.882	1.268
0.25	0.98765	0.96942	2.403	0.95745	2.300	1.042
0.30	0.98232	0.95638	2.035	0.93947	1.912	0.89699
0.35	0.97609	0.94128	1.778	0.91877	1.634	0.79738
0.40	0.96899	0.92427	1.590	0.89561	1.424	0.72632
0.45	0.96108	0.90551	1.449	0.87027	1.261	0.67423
0.50	0.95238	0.88517	1.340	0.84302	1.130	0.63535
0.55	0.94295	0.86342	1.255	0.81417	1.022	0.60602
0.60	0.93284	0.84045	1.188	0.78400	0.93155	0.58377
0.65	0.92208	0.81644	1.136	0.75283	0.85493	0.56692
0.70	0.91075	0.79158	1.094	0.72093	0.78896	0.55425
0.75	0.89888	0.76604	1.062	0.68857	0.73155	0.54485
0.80	0.88652	0.73999	1.038	0.65602	0.68110	0.53807
0.85	0.87374	0.71361	1.021	0.62351	0.63640	0.53338

copyright ©, 2007, by Dr. Bar-Meir

www.potto.org

Table 4.2 Gas Dynamic Table for subsonic flow

Table 1.3: Isentropic Flow for  $k=1.4$  (continue)

M	$\frac{T}{T_0}$	$\frac{\rho}{\rho_0}$	$\frac{A}{A^*}$	$\frac{P}{P_0}$	$\frac{A \times P}{A^* \times P_0}$	$\frac{F}{F^*}$
0.90	0.86059	0.68704	1.009	0.59126	0.59650	0.53039
0.95	0.84710	0.66044	1.002	0.55946	0.56066	0.52877
1.0	0.83333	0.63394	1.000	0.52828	0.52828	0.52828
1.05	0.81934	0.60765	1.002	0.49787	0.49888	0.52871
1.10	0.80515	0.58170	1.008	0.46835	0.47207	0.52989
1.15	0.79083	0.55616	1.017	0.43983	0.44751	0.53169
1.20	0.77640	0.53114	1.030	0.41238	0.42493	0.53399
1.25	0.76190	0.50670	1.047	0.38606	0.40411	0.53670
1.30	0.74738	0.48290	1.066	0.36091	0.38484	0.53974
1.35	0.73287	0.45980	1.089	0.33697	0.36697	0.54305
1.40	0.71839	0.43742	1.115	0.31424	0.35036	0.54655
1.45	0.70398	0.41581	1.144	0.29272	0.33486	0.55022
1.50	0.68966	0.39498	1.176	0.27240	0.32039	0.55401
1.55	0.67545	0.37495	1.212	0.25326	0.30685	0.55788
1.60	0.66138	0.35573	1.250	0.23527	0.29414	0.56182
1.65	0.64746	0.33731	1.292	0.21839	0.28221	0.56578
1.70	0.63371	0.31969	1.338	0.20259	0.27099	0.56976
1.75	0.62016	0.30287	1.386	0.18782	0.26042	0.57373
1.80	0.60680	0.28682	1.439	0.17404	0.25044	0.57768
1.85	0.59365	0.27153	1.495	0.16119	0.24102	0.58161
1.90	0.58072	0.25699	1.555	0.14924	0.23211	0.58549
1.95	0.56802	0.24317	1.619	0.13813	0.22367	0.58932
2.00	0.55556	0.23005	1.688	0.12780	0.21567	0.59309
2.25	0.49689	0.17404	2.096	0.086482	0.18130	0.61095
2.50	0.44444	0.13169	2.637	0.058528	0.15432	0.62693

Table 4.3 Gas Dynamic Table for supersonic

When we compare our theoretical values with gas dynamic table, we see that Mach number is in the incompressible region in Table 4.2. In fluid mechanics or more generally continuum mechanics, incompressible flow (isochoric flow) refers to a flow in which the material density is constant within a fluid parcel—an infinitesimal volume that moves with the flow velocity. An equivalent statement that implies incompressibility is that the divergence of the flow velocity is zero. Incompressible flow does not imply that the fluid itself is incompressible. Incompressible flow implies that the density remains constant within a parcel of fluid that moves with the flow velocity. A homogeneous, incompressible material is one that has constant density throughout.

Incompressible flow:  $\nabla \cdot v = 0$  This can assume either constant density (strict incompressible) or varying density flow. The varying density set accepts solutions involving small perturbations in density, pressure and/or temperature fields, and can allow for pressure stratification in the domain.

According to Mach number 0.145, we need to calculate our value on the gas dynamic table via interpolation method because we do not have a direct value from a gas dynamic table.

Interpolation;

Ma	T0/T	Q0/Q	P0/P	A0/A
0.1	1.002	1.005	1.007	5.822
<b>0.145</b>	<b>1.0047</b>	<b>1.01175</b>	<b>1.01645</b>	<b>4.5359</b>
0.2	1.008	1.02	1.028	2.964

Table 4.2 For Mach number 0.145 values

#### 4.1.3 Mass flow rate of the system and outlet velocity of the test section

Inlet and outlet of the test section should be equal (equation 2.4);

$$\frac{\Delta m}{\Delta t} = q_1 * A_1 * v_1 = q_2 * A_2 * v_2$$

$$1.226 * 3.14 * 26.6 = 1.226 * 9.878 * V_2$$

$$V_{outlet} = V_2 = 8.45 \text{ m/s}$$

Given and calculated values;

Test Section locations	q-density	A-area	V-velocity
inlet	1.226 kg/m <sup>3</sup>	3.14 m <sup>2</sup>	26.6 m/s
outlet	1.226 kg/m <sup>3</sup>	9.878 m <sup>2</sup>	8.45 m/s

System inlet is located at nozzle inlet and we consider to calculate the mass flow rate of the system through inlet area and velocity.

$$\dot{m} = q * v_{inlet \text{ of the nozzle}} * A$$

$$\dot{m} = 1.226 * 6.9 * (3.9129 * 3.14)$$

$$\dot{m} = 103.9 \text{ kg/s}$$

#### 4.1.4 Hydraulic diameter and Reynold's number at Critical location

The hydraulic diameter,  $D_H$ , is a commonly used term when handling flow in non-circular tubes and channels. Using this term, one can calculate many things in the same way as for a round tube. It is defined as;

$$D_h = \frac{4A}{P_e} \quad (4.0)$$

Where,

$A$  is the cross-sectional area of the flow,

$P_e$  is the wetted perimeter of the cross-section.

More intuitively, the hydraulic diameter can be understood as a function of the hydraulic radius  $R_H$ , which is defined as the cross-sectional area of the channel divided by the wetted perimeter.

The need for the hydraulic diameter arises due to the use of a single dimension in case of dimensionless quantity such as Reynolds number, which prefers a single variable for flow analysis rather than the set of variables as listed in the table. The Manning formula contains a quantity called the hydraulic radius. Despite what the name may suggest, the hydraulic diameter is not twice the hydraulic radius, but four times larger.

Hydraulic diameter is mainly used for calculations involving turbulent flow. Secondary flows can be observed in non-circular ducts as a result of turbulent shear stress in the turbulent flow. Hydraulic diameter is also used in the calculation of heat transfer in internal-flow problems.

Geometry

Hydraulic Diameter

Circular

$$D_h = \frac{4 \cdot \frac{D^2}{4}}{\pi \cdot D} = D \quad (4.1)$$

Rectangular

$$D_h = \frac{4 \cdot a \cdot b}{2 \cdot (a+b)} = \frac{2 \cdot a \cdot b}{a+b} \quad (4.1.1)$$

Nozzle Hydraulic Diameter;

According to equation 4.1 Nozzle Hydraulic Diameter is equal to diameter of inlet and outlet of the nozzle because the nozzle has circular inlet and outlet.

Test Section Hydraulic Diameter;

As we know our design of test section as a rectangular shape and we consider equation (4.1),

Nozzle outlet and Test section inlet are the same locations so do not necessary to calculate again. This is equal to diameter of outlet of the nozzle.

Due to the outlet of the test section;

$$Dh = \frac{4*a*b}{2*(a+b)} = \frac{2*a*b}{a+b} = \frac{2*3.556*2.778}{3.556+2.778}$$

$$Dh = 3.12 \text{ m}$$

Reynold's number at critical locations;

Due to the inlet section of the nozzle, we use equation (2.12) so,

$$Re = \frac{q*v_{inlet}*Dh}{\gamma} = \frac{v_{inlet}*Dh}{\nu}$$

$$Re = \frac{6.9*3.96}{1.516*10^{-5}}$$

$$Re = 1802300$$

Due to the outlet section of the nozzle, we use equation (2.12) so,

$$\text{Re} = \frac{q \cdot v_{\text{outlet}} \cdot D_h}{\mu} = \frac{v_{\text{outlet}} \cdot D_h}{\nu}$$

$$\text{Re} = \frac{26.66 \cdot 2}{1.516 \cdot 10^{-5}}$$

$$\text{Re} = 3517000$$

Due to the outlet section of the test section, we use equation (2.12) so;

$$\text{Re} = \frac{q \cdot v_{\text{outlet}} \cdot D_h}{\mu} = \frac{v_{\text{outlet}} \cdot D_h}{\nu}$$

$$\text{Re} = \frac{8.45 \cdot 3.12}{1.516 \cdot 10^{-5}}$$

$$\text{Re} = 1739000$$

We identified flow situations all critical sections these are inlet of the nozzle, outlet of the nozzle and outlet of the system via Reynold's number. Reynold's values of all of sections are bigger than 4000 and it means these are in turbulent flow condition.

## CHAPTER 5

### MODEL OF GEOMETRY

These design graphs show the specific dimensions from the top, front of the wind tunnel, and the contraction cone as well. The length and degree units of these three design graphs are in inches and degree. The software that was used was the Solidworks student version. Solidworks is commercial software that can be utilized for 2D and 3D computer-aided design (CAD) and drafting—it has been available since 1982 as a desktop application and since 2010 as a mobile web- and cloud-based app marketed

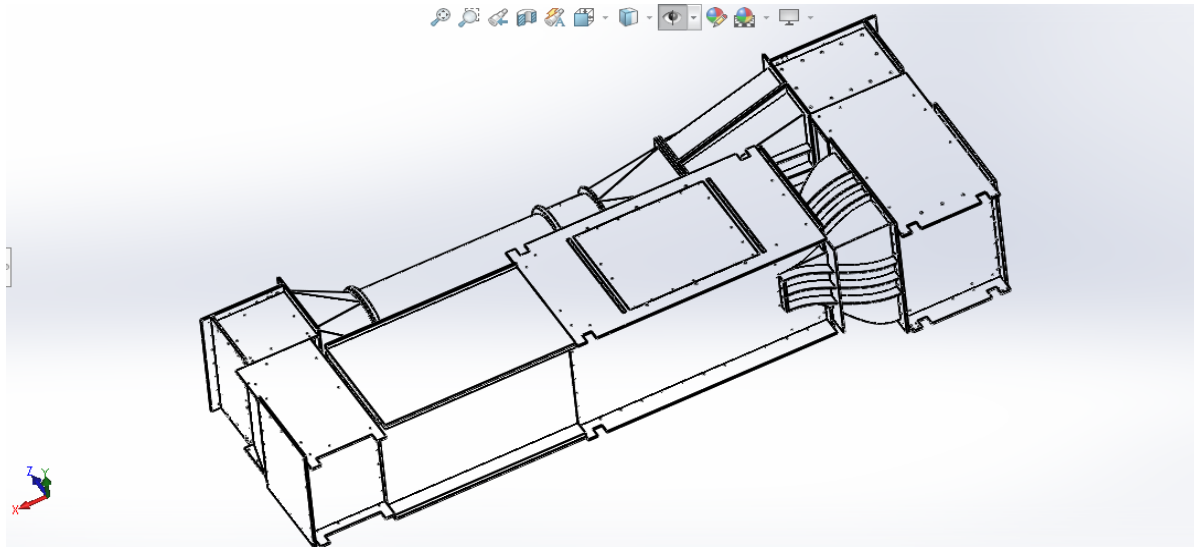


*Figure 5 Model of the wind tunnel system*

Above in picture 5 shows all parts are assembled, as we can see in figure the wind tunnel complicated design because of the drawing contains all details as screws, assemblies, supports, aluminum plates, etc.

According to our aim, we consider getting details located at nozzle and testing area sections. For analysis of the testing section within the nozzle, we have to redesign with same measurements to make simplify style of these parts because of sections have extra solid parts and impossible to do fluid analysis.

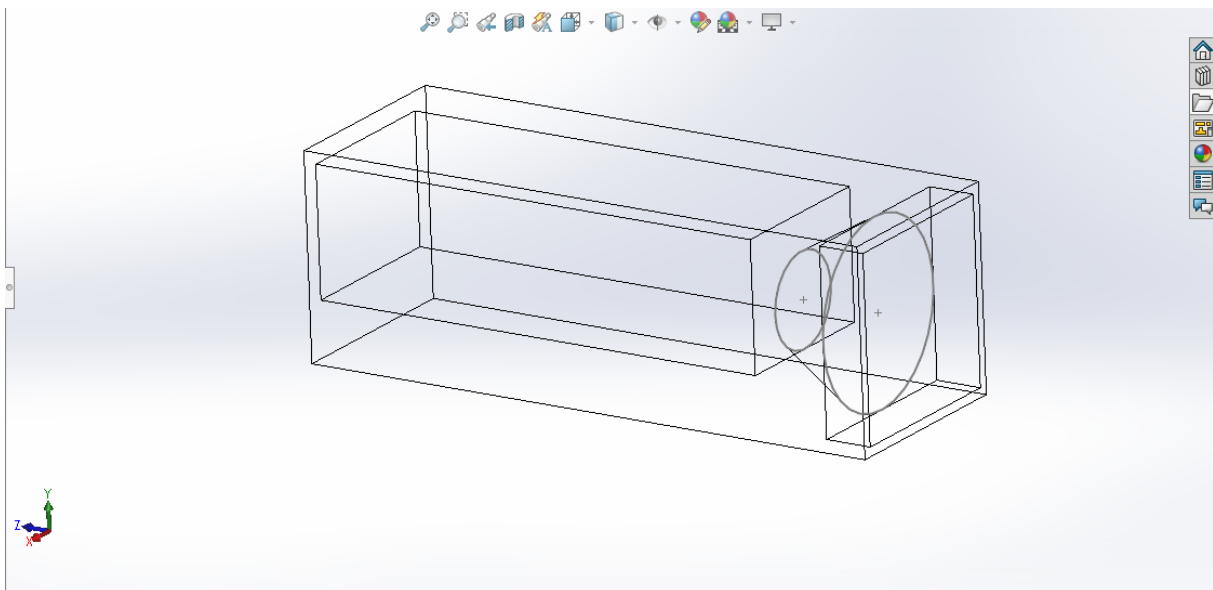


*Figure 5.1 model detail of the wind tunnel system*



I would describe to investigation model, representing the system. The left side is the outlet section of the system, air goes from nozzle to testing area (right side of the figure 5.1) and there is a support plane under the model. Full system was designed, designed with SolidWorks.

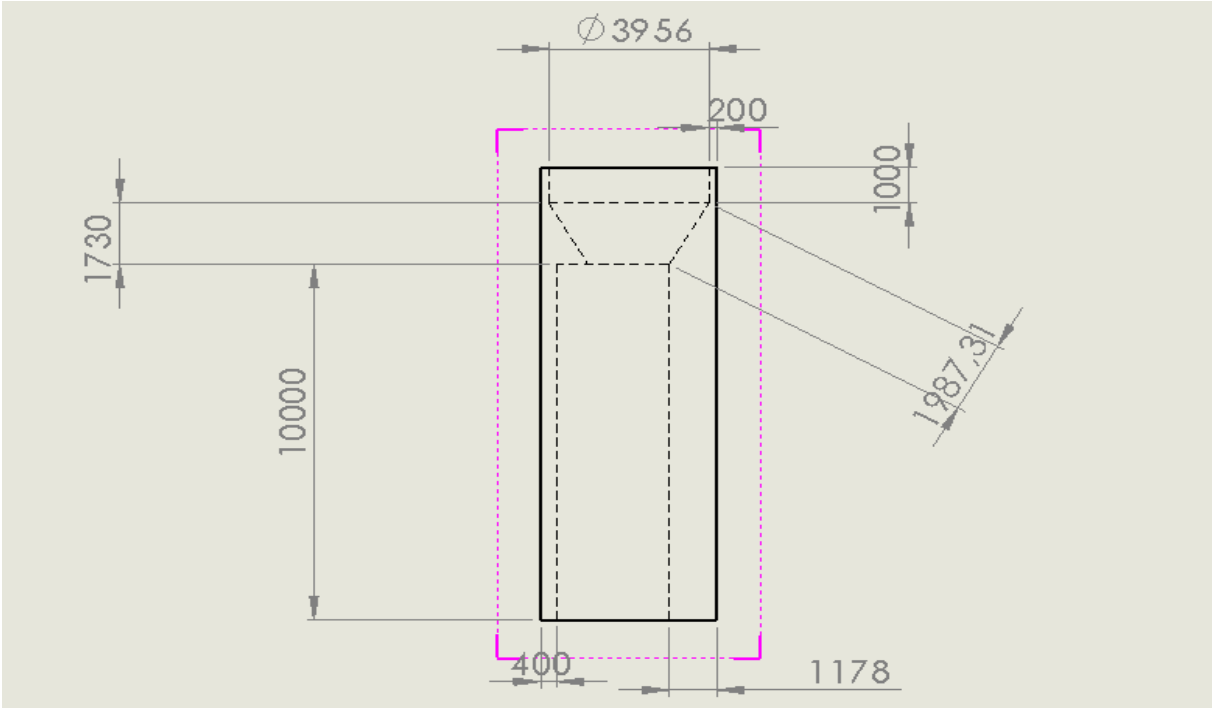


Figure 5.2 Technical drawing of the model on top view

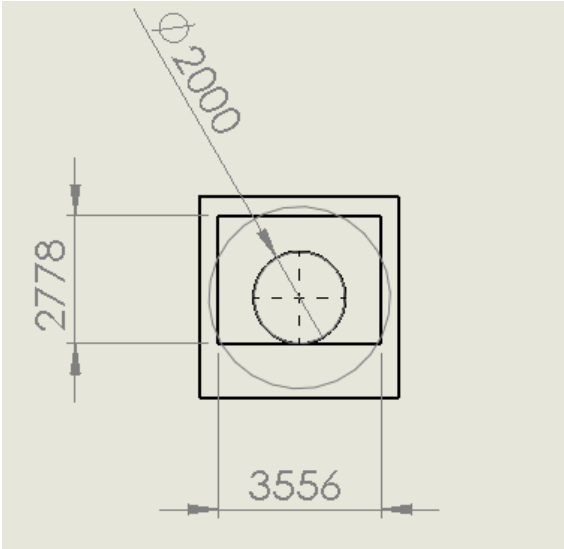


Figure 5.3 Technical draw of in front view

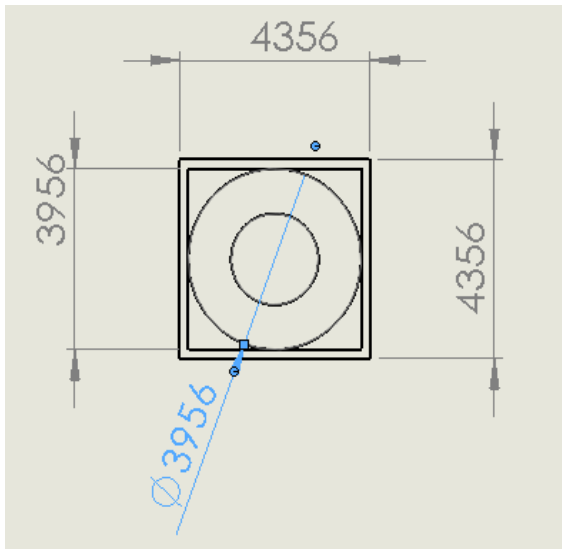


Figure 5.4 Technical draw of back side

# CHAPTER 6

## ANALYSIS OF THE SYSTEM

Due to analysis of the wind tunnel system, I preferred to use Ansys Fluent software because of Fluent software contains the broad, physical modeling capabilities needed to model flow, turbulence, heat transfer and reactions for industrial applications. These range from air flow over an aircraft wing to combustion in a furnace, from bubble columns to oil platforms, from blood flow to semiconductor manufacturing and from clean room design to wastewater treatment plants. Fluent spans an expansive range, including special models, with capabilities to model in-cylinder combustion, aero-acoustics, and turbomachinery and multiphase systems. The software helps to solve and identify problems for heat transfer, fluid flow and mass transport via based on the finite element method. This so hard and so much consuming time to calculate which boundary value problems for partial differential equations. Ansys Cfd and Fluent use variation methods from the calculus of variations to approximate a solution by minimizing an associate error function.

### 6.1 Preparation for analysis

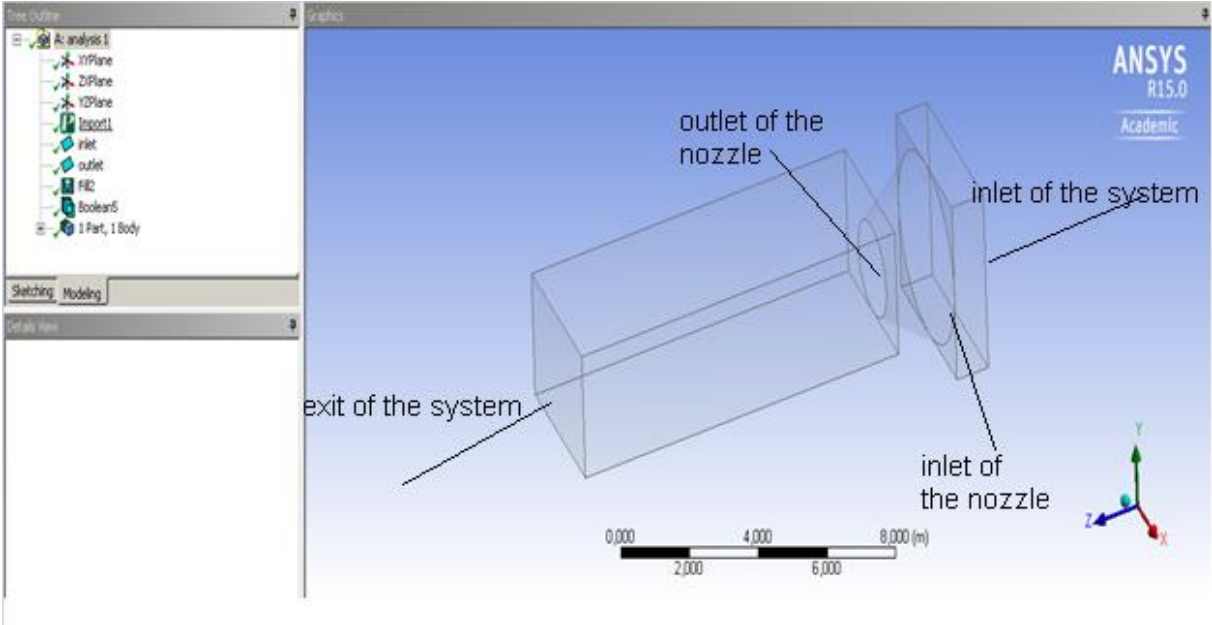


Figure 6 Preparation of analysis

### 6.1.1 Geometry Preparation

- Surface From Edge

The Surfaces from Edges feature allows the creation of Surface bodies in ANSYS Design Modeler that use existing body edges, including Line body edges as the boundary. Edges should be chosen such that they produce non-intersecting closed loops. Each closed loop will create a frozen surface body that contains a single face. The loops should form a shape such that a simple surface can be inserted into the model. Examples of simple surfaces are planes, cylinders, tori, cones, and spheres. Simply ruled surfaces can also be created. After a surface has been generated, you can choose to flip the normal of the surface by setting Flip Surface Normal to Yes (INC., 2012).

- Fill Using By Caps Method

This method is used to extract inverse volumes enclosed by one or more bodies in a model. For example, if you want to do a CFD analysis of the heat exchanger on a tube side as shown in the image below, you can create the geometry that represents the fluid by using this method. First cap the inlet and outlet of the tube by creating Surface bodies. Then select the Solid bodies that represent the tube. On generate, a frozen body will be created that represents the inverse volume (Lockwood, 2015).

- Boolean Subtract section

Boolean feature is used to Unite, Subtract, Intersect, or Imprint Faces of existing bodies. The bodies can be Solid, Surface, or (for Unite only) Line bodies.

- Fluid Flow

Fluent allows for a fluid flow analysis of incompressible and compressible fluid flow and heat transfer in complex geometries. You specify the computational models, materials, boundary conditions, and solution parameters in Fluent, where the cases are solved. You can use a Fluent fluid flow analysis system to apply a computational mesh to a geometry within Workbench, then use Fluent to define pertinent mathematical models (e.g., low-speed, high-speed, laminar, turbulent, etc.), select materials, define boundary conditions, and specify solution controls that best represent the problem to be solved. Fluent solve the mathematical equations, and the results of the simulation can be displayed in Fluent or in CFD-Post for further analysis (e.g. contours, vectors, etc.) (INC., 2012).

### 6.1.2 Mesh

The meshing of the wind tunnel, the meshing of the parts are done so that we can brief view of the part we designed and the parameters that we are going to compute in the future using solver as in my case is the velocity. In order to get the good quality which is "Tetrahedrons (Patch Conforming) Method was used to reach regular and pure mesh quality was selected.

Scaling (**Grid Independence**) Test, grid convergence is the term used to describe the improvement of results by using successively smaller cell sizes for the calculations. A calculation should approach the correct answer as the mesh becomes finer, hence the term grid convergence. The simulation on progressively finer grids (3 grids should be at least) by changing element size between 2 and 2.5 times refinement. Therefore 3 different mesh were chosen and simulated. 3 types of application to get proper values as much as desirable and these types of application represent about 2.2 grow up for becoming mesh elements are as 54112, 113555 and 202153 respectively. Mesh elements constitute within edge sizing and inflation layer.

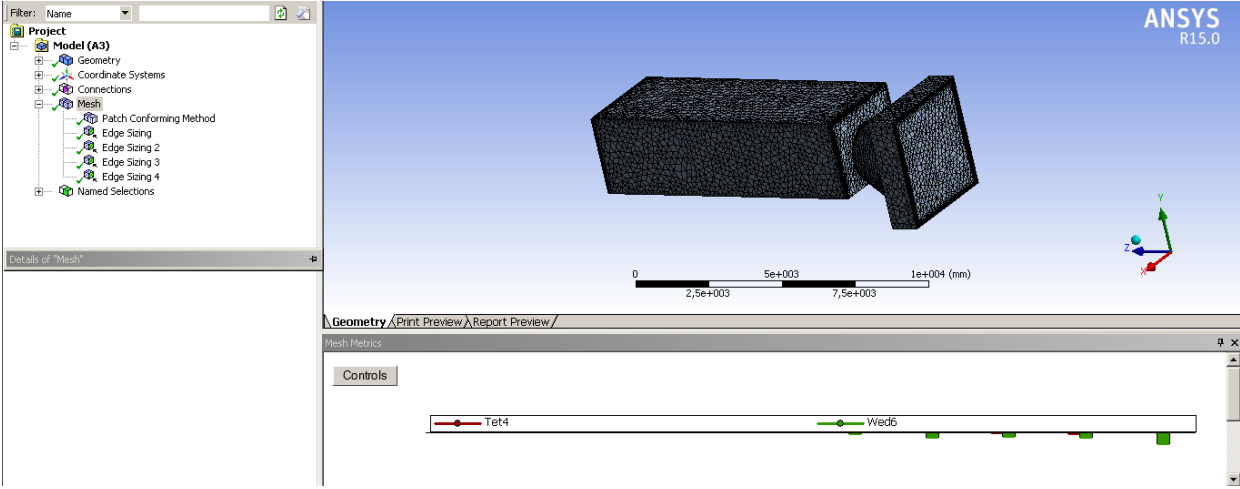


Figure 6.1 Mesh Illustration of general system

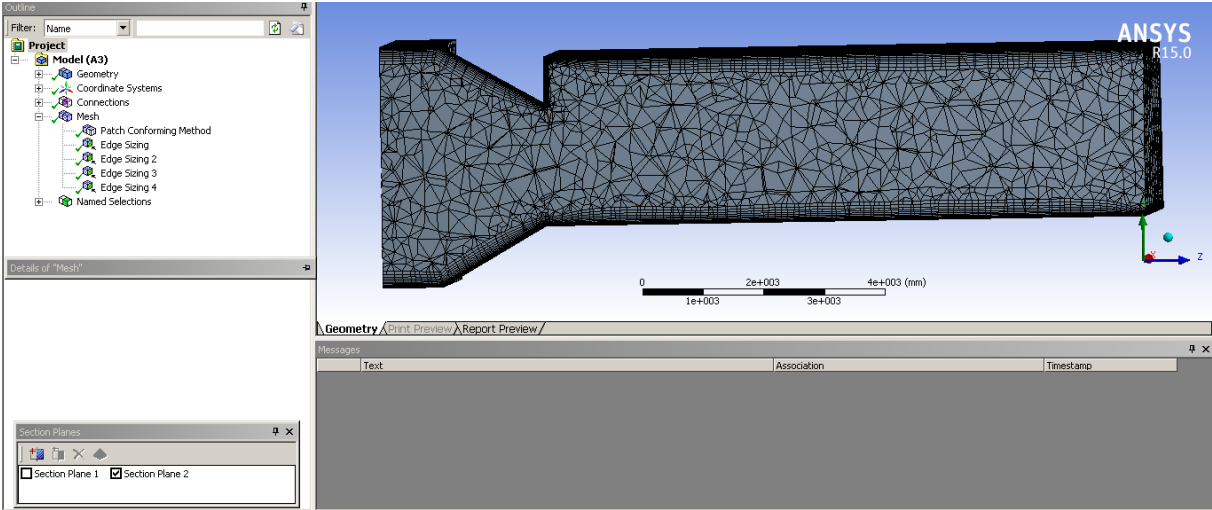


Figure 6.2 Section Plane shows inflation layers of the system

- *Orthogonal quality* is computed for cells using the vector from the cell centroid to each of its faces, the corresponding face area vector, and the vector from the cell centroid to the centroids of each of the adjacent cells. The worst cells will have an orthogonal quality closer

to 0, with the best cells closer to 1. The minimum orthogonal quality for all types of cells should be more than 0.01, with an average value that is significantly higher.

- *Skewness* is defined as the difference between the shape of the cell and the shape of an equilateral cell of equivalent volume. Highly skewed cells can decrease accuracy and destabilize the solution. A general rule is that the maximum skewness for a triangular/tetrahedral mesh in most flows should be kept below 0.95, with an average value that is significantly lower. A maximum value above 0.95 may lead to convergence difficulties and may require changing the solver controls, such as reducing under-relaxation factors and/or switching to the pressure-based coupled solver.

Statistics	
Bodies	1
Active Bodies	1
Nodes	93582
Elements	202153
Mesh Metric	Orthogonal Quality
Min	0,087749609578057
Max	0,999706864154866
Average	0,80175585105277
Standard Deviation	0,145230178831411

Figure 6.3 First application orthogonal quality

Statistics	
Bodies	1
Active Bodies	1
Nodes	93582
Elements	202153
Mesh Metric	Skewness
Min	1,17340914941189E-03
Max	0,96250196163151
Average	0,33896165401939
Standard Deviation	0,160106833095613

Figure 6.4 First application skewness

Figure 6.3 and 6.4 show minimum orthogonal quality is  $0.0877 < 0.1$  and maximum skewness quality is  $0.96 > 0.95$ . These are not very good values but element number is so high for that complex shape.

Statistics	
Bodies	1
Active Bodies	1
Nodes	49489
Elements	113555
Mesh Metric	Orthogonal Quality
Min	0,101894342432252
Max	0,999646814604325
Average	0,853777151365544
Standard Deviation	0,123680524475721

Figure 6.5 Second application orthogonal quality

Statistics	
Bodies	1
Active Bodies	1
Nodes	49489
Elements	113555
Mesh Metric	Skewness
Min	1,7499640506583E-03
Max	0,950316889974096
Average	0,294351297302103
Standard Deviation	0,162007196272894

Figure 6.6 Second application skewness

Figure 6.5 and 6.6 show minimum orthogonal quality is  $0.101894 < 0.1$  and maximum skewness quality is  $0.9503 > 0.95$ . These are good values but element number is not so high to reach good results for that complex shape.

Statistics	
Bodies	1
Active Bodies	1
Nodes	14766
Elements	54112
Mesh Metric	Orthogonal Quality
Min	0,13100840800479
Max	0,998899633309342
Average	0,836284898303211
Standard Deviation	9,57094937360064E-02

Figure 6.7 Third application orthogonal quality

Statistics	
Bodies	1
Active Bodies	1
Nodes	14766
Elements	54112
Mesh Metric	Skewness
Min	3,25360749574011E-04
Max	0,950316444149239
Average	0,28329038512547
Standard Deviation	0,147272876157498

Figure 6.8 Third application skewness

Figure 6.7 and 6.8 show minimum orthogonal quality is  $0.13100 < 0.1$  and maximum skewness quality is  $0.9503 > 0.95$ . These are better than other values but element number is so less for that complex shape and results may be far away from reality.

According to statistics of 3 different type analysis, the first application (element number 202153) has highest element number and close suitable mesh statistics within legal limits.

### 6.1.3 Fluent Solver

It was used ANSYS fluent solver which was set up as a condition of pressure based and we use k-epsilon (2 eqn.) for models. Also, our main actor is air as a fluid in the system. Inlet conditions are considered as a boundary condition to analysis to our system.

Reference values for fluent solver respectively;

- Area=1m<sup>2</sup> (which is used to compute the force and moment coefficients)
- Density of Air=1.225 kg/m<sup>3</sup> (compute the reference dynamic pressure)
- Enthalpy=0 (determine the total enthalpy change)
- Length=1m (computation of the moment coefficient)
- Pressure =0 pa (pressure-related forces and moments and the pressure coefficient)
- Temperature=298.15 K (compute entropy for incompressible flows)
- Inlet Velocity of the system=5.5 m/s (calculated by theoretical formula)
- Viscosity=1.7894\*10<sup>-5</sup> (the boundary Reynolds number)
- The ratio of specific heats=1.4

Inlet velocity applied throughout Z direction. Specification method chooses Intensity and Viscosity ratio. Turbulent Intensity is % 5, Turbulent Viscosity ratio is the boundary value for the modified turbulent viscosity,  $\tilde{\nu}$  and by combining  $\frac{\mu_t}{\mu}$  with the appropriate values of density and molecular viscosity which is 10. Wall motion applied as Stationary Wall and Shear condition is no slip. Wall roughness constant shows 0.5.

Solution method;

Scheme	SIMPLE
Gradient	LEAST SQUARES CELL BASED
Pressure	SECOND ORDER
Momentum	SECOND ORDER UPWIND
Turbulent Kinetic Energy	SECOND ORDER UPWIND
Turbulent Dissipation Rate	SECOND ORDER UPWIND

It was used implicit solution method and calculated 3000 iterations which converged to according to converge criteria is  $10^{-6}$ . Critical locations values were tabulated as inlet of the system, inlet of the nozzle, outlet of the nozzle and outlet of the system as well as element size. 4 tables were prepared to show mean velocities, total pressures, dynamic pressures and absolute pressures

Element Size	Inlet Velocity of the system	Inlet Velocity of the nozzle	Outlet Velocity of the nozzle	Outlet Velocity of the system
202153	5.5 m/s	6.0873241 m/s	27.589312 m/s	8.7011585 m/s
54112	5.5 m/s	6.9571471 m/s	27.46284 m/s	8.87911161 m/s
113555	5.5 m/s	7.0133114 m/s	29.062473 m/s	9.1564665 m/s

*Table 4.2 Mean Velocity results of the analysis*

Element Size	Inlet Total pressure of the system	Inlet Total pressure of the nozzle	Outlet Total pressure of the nozzle	Outlet Total pressure of the system
202153	902.34 pascal	898.38 pascal	694.22 pascal	69.9 pascal
54112	525.07 pascal	528.20 pascal	531.51 pascal	80.45 pascal
113555	645.88 pascal	649.53 pascal	674.02 pascal	90.13 pascal

*Table 4.3 Total pressure of the system*



Element Size	Inlet Dynamic pressure of the system	Inlet Dynamic pressure of the nozzle	Outlet Dynamic pressure of the nozzle	Outlet Dynamic pressure of the system
202153	18.49 pascal	30.55 pascal	502.34 pascal	64.24 pascal
54112	18.53 pascal	31.99 pascal	464.43 pascal	80.88 pascal
113555	18.53 pascal	32.48 pascal	520.75 pascal	90.69 pascal

*Table 4.4 Dynamic pressure of the system*

Element Size	Inlet Absolute pressure of the system	Inlet Absolute pressure of the nozzle	Outlet Absolute pressure of the nozzle	Outlet Absolute pressure of the system
202153	102208 pascal	102192 pascal	101516 pascal	101325 pascal
54112	101831 pascal	101821 pascal	101392 pascal	101324 pascal
113555	101952 pascal	101942 pascal	101478 pascal	101324 pascal

*Table 4.5 Absolute pressure of the system*

Tables show element size, inlet velocity of the system, inlet velocity of the nozzle, outlet velocity of the nozzle, and outlet velocity as well as pressure conditions of the system respectively. When we compare our theoretical values within analysis table value, I would like to consider element size which has 202153(first application) number element size due to reach a reasonable final solution because the first application has the nearest values with my theoretical values.

#### 6.1.4 Pressure and Velocity Profile of the system

The profile of velocity not only shows you the magnitude of velocity but also shows you the characteristics of the flow like direction, change due to the shape of the domain or increase-decrease in the velocity magnitude with respect to the geometry and so on. So in general, it helps you to understand how the fluid behaves while it is transported through the domain.

Pressure Profile is exerted between two items that are in contact with one another. The Pressure Profile is the pressure distribution over the entire contact area. For a static situation, such as two items bolted together, pressure does not change with time.

As we focus to evaluate values which are from the first application so Illustrations are used from the first application.

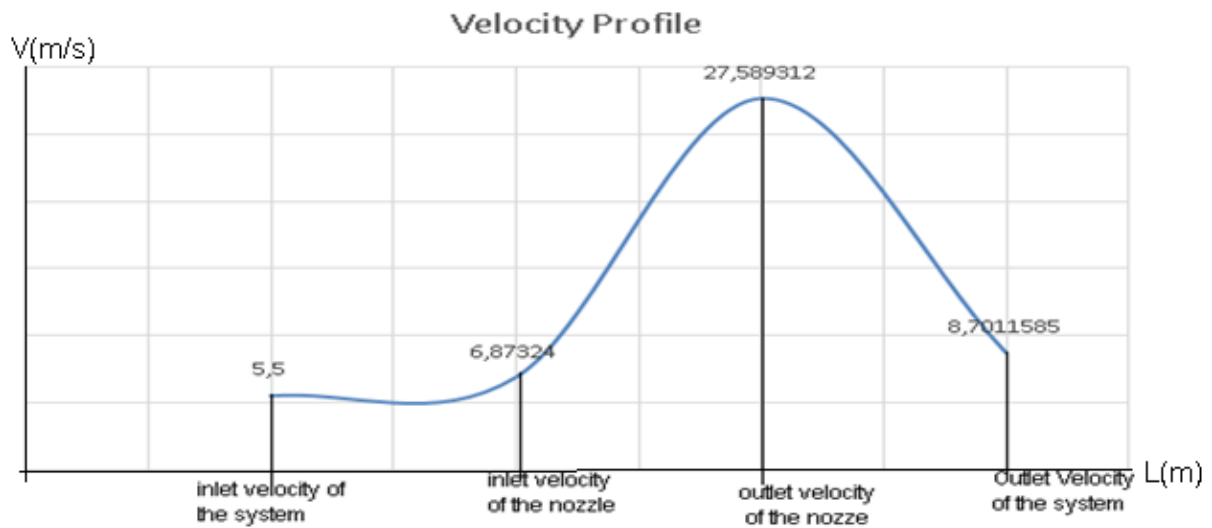


Figure 6.9 Velocity graph of overall system (m/s)

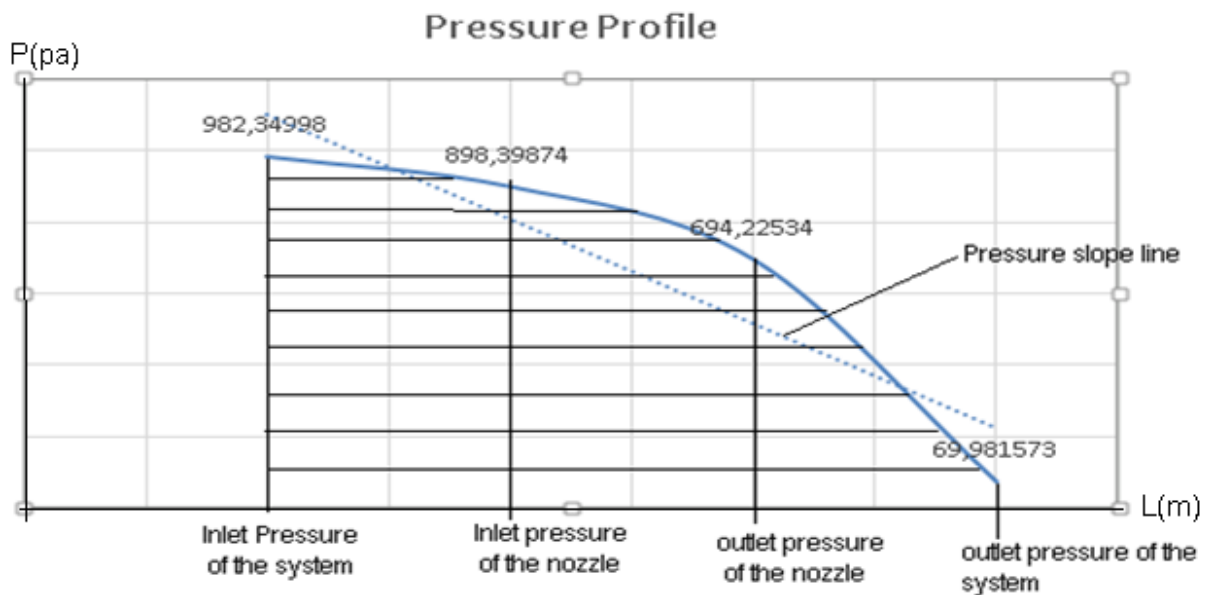


Figure 6.9.1 Total Pressure graph of overall system (Pascal)

## 6.2 Grid Analysis

The Grid is an apparatus to provide more regular flow with the desired velocity because the flow pressure cannot be changed without velocity changes when the flow profile goes to become irregular and also reach to any pressure profile via grid plate which is adjustable to arrange according to our needs.

6.2.1 Model of Grid

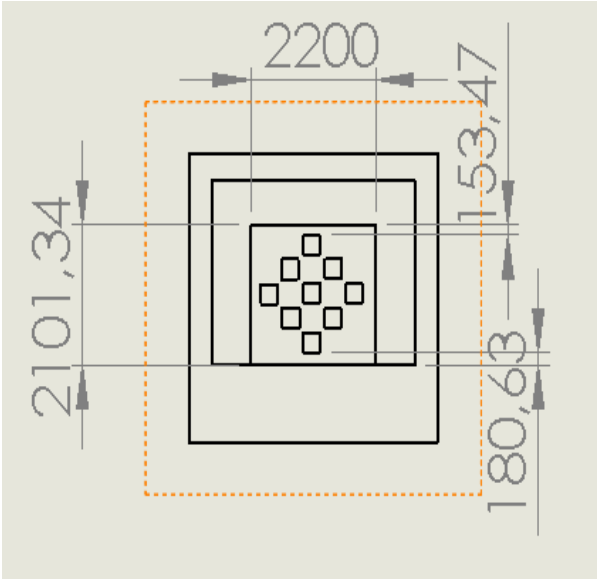


Figure 7 Front side of Grid

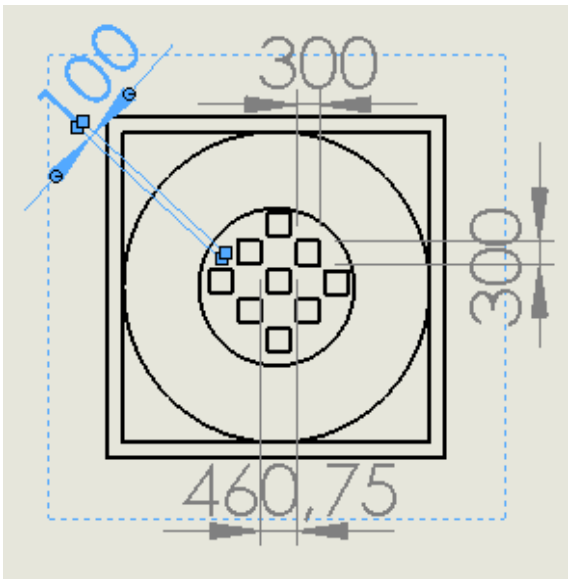


Figure 7.1 Back side of Grid

The special design grid used that is given for the system, the grid was modelled with 9 rectangular holes and holes were echeloned as star style on the cylindrical plate. Holes measurements are 300mm\*300mm and Plate has 2200mm length\* 2101, 34mm height. Each hole are located between 100mm one another and the grid assembled on the exit of the nozzle.

6.2.2 Mesh of the model with normal grid

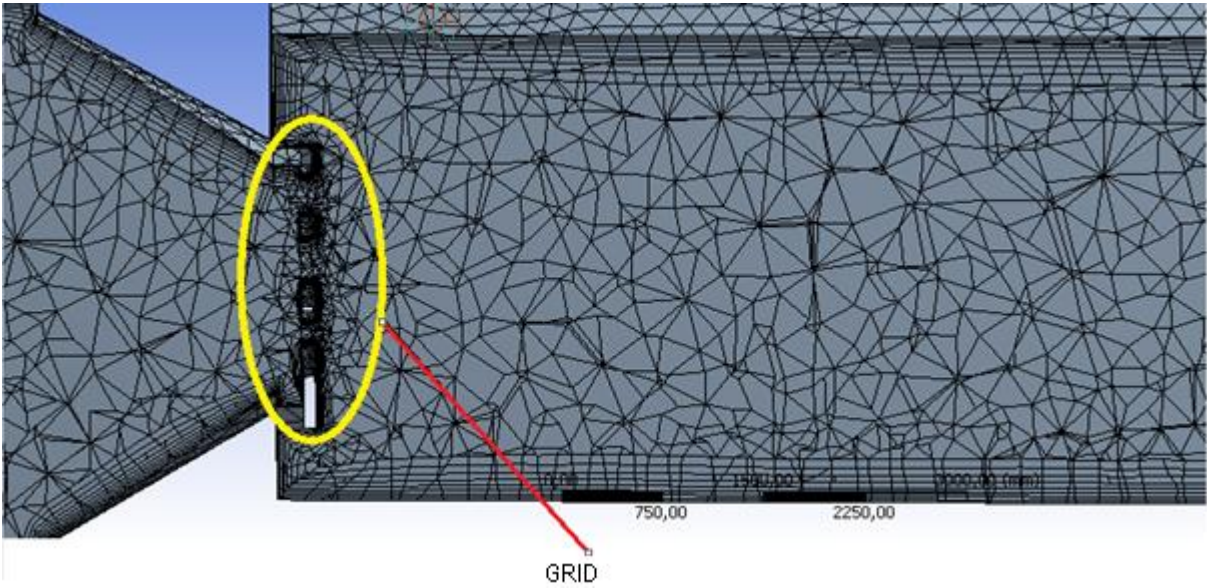


Figure 7.2 Grid illustration with inflation layers

The meshing of the model with grid, the meshing of the parts is done so that we can brief view of the part we designed and the parameters that we are going to compute in the future using

solver as in my case is the velocity. In order to get the good quality which was selected ‘‘Tetrahedrons (Patch Conforming) Method’’ used to reach regular and pure mesh quality.

I try to catch good orthogonal and skewness quality so I applied one operation for the grid.

Statistics	
Bodies	1
Active Bodies	1
Nodes	56560
Elements	133170
Mesh Metric	Orthogonal Quality
Min	0,028155472138205
Max	0,99978624719136
Average	0,809848618067453
Standard Deviation	0,162961221947198

Figure 7.3 Grid analysis orthogonal quality

Statistics	
Bodies	1
Active Bodies	1
Nodes	56560
Elements	133170
Mesh Metric	Skewness
Min	2,59387104817632E-03
Max	0,950316889974096
Average	0,33505379376656
Standard Deviation	0,177363955097906

Figure 7.4 Grid analysis Skewness

Figure 7.3 and 7.4 show minimum orthogonal quality is  $0.0281 < 0.1$  and maximum skewness quality is  $0.9503 > 0.95$ . These are good values to analyze with that element number.

### 6.2.3 Fluent Solver

The used of ANSYS fluent solver which was set up as a condition of density based and we use k-epsilon (2 eqn.) for models. Also, our main actor is air as a fluid in the system. Inlet conditions are considered as a boundary condition to analysis to our system.

Reference values for fluent solver respectively;

- Area= $1\text{m}^2$  (which is used to compute the force and moment coefficients)
- Density of Air= $1.225\text{ kg/m}^3$  (compute the reference dynamic pressure)
- Enthalpy= $0$  (determine the total enthalpy change)
- Length= $1\text{m}$  (computation of the moment coefficient)
- Pressure = $0\text{ pa}$  (pressure-related forces and moments and the pressure coefficient)
- Temperature= $298.15\text{ K}$  (compute entropy for incompressible flows)

- Inlet Velocity of the system=5.5 m/s (calculated by theoretical formula)
- Viscosity=1.7894\*10<sup>-5</sup> (the boundary Reynolds number)
- The ratio of specific heats=1.4

Inlet velocity applied throughout Z direction. Specification method chooses Intensity and Viscosity ratio. Turbulent Intensity is % 5, Turbulent Viscosity ratio is the boundary value for the modified turbulent viscosity,  $\tilde{\nu}$  and by combining  $\frac{\mu_t}{\mu}$  with the appropriate values of density and molecular viscosity which is 10. Wall motion applied as Stationary Wall and Shear condition is no slip. Wall roughness constant shows 0.5.

Solution method;

Scheme	SIMPLE
Gradient	LEAST SQUARES CELL BASED
Pressure	SECOND ORDER
Momentum	SECOND ORDER UPWIND
Turbulent Kinetic Energy	SECOND ORDER UPWIND
Turbulent Dissipation Rate	SECOND ORDER UPWIND

We use implicit solution method as well as calculated 3000 iterations with converged to calculation according to my converge criteria is 10<sup>-6</sup>. Critical locations values were tabulated as inlet of the system, inlet of the nozzle, outlet of the nozzle and outlet of the system as well as element size. 4 tables were prepared to show mean velocities, total pressures, dynamic pressures and absolute pressures

Element size	Inlet Velocity of the system	Inlet Velocity of the nozzle	Outlet Velocity of the nozzle	Outlet velocity of the system
133170	5.5 m/s	6.99 m/s	29.14 m/s	9.71 m/s
284221	5.5 m/s	6.98 m/s	26.39 m/s	10.61 m/s
62126	5.5 m/s	6.93 m/s	23.30 m/s	9.58 m/s

Table 4.3 Mean Velocity values of the grid system

Element size	Inlet Pressure of the system	Total pressure of the nozzle	Outlet pressure of the nozzle	Total pressure of the system
133170	11732 pascal	11736 pascal	347.51 pascal	97.53 pascal
284221	12037 pascal	12041 pascal	160.81 pascal	92.15 pascal
62126	10503 pascal	10506 pascal	389.51 pascal	90.62 pascal

Table 4.3 Total pressure of the grid system

Element size	Inlet Dynamic Pressure of the system	Inlet Dynamic pressure of the nozzle	Outlet Dynamic pressure of the nozzle	Outlet Dynamic pressure of the system
133170	18.51 pascal	32.33 pascal	1281.37 pascal	100.44 pascal

284221	18.53 pascal	32.18 pascal	1196.23 pascal	94.42 pascal
62126	18.53 pascal	31.77 pascal	994.41 pascal	93 pascal

Table 4.4 Dynamic pressure of the grid system

Element Size	Inlet Absolute Pressure of the system	Inlet Absolute pressure of the nozzle	Outlet Absolute pressure of the nozzle	Outlet Absolute pressure of the system
133170	113039 pascal	113029 pascal	100391 pascal	101323 pascal
284221	113344 pascal	113333 pascal	100289 pascal	101324 pascal
62126	107811 pascal	107806 pascal	100834 pascal	101324 pascal

Table 4.5 Absolute pressure of grid system

Tables' shows element size, inlet velocity of the system, inlet velocity of the nozzle, outlet velocity of the nozzle, and outlet velocity as well as pressure conditions of the system respectively. When we compare our theoretical values within analysis table value, I would like to consider element size which has 133170(first application) number element size due to reach a reasonable final solution because the first application has the nearest values with my theoretical values.

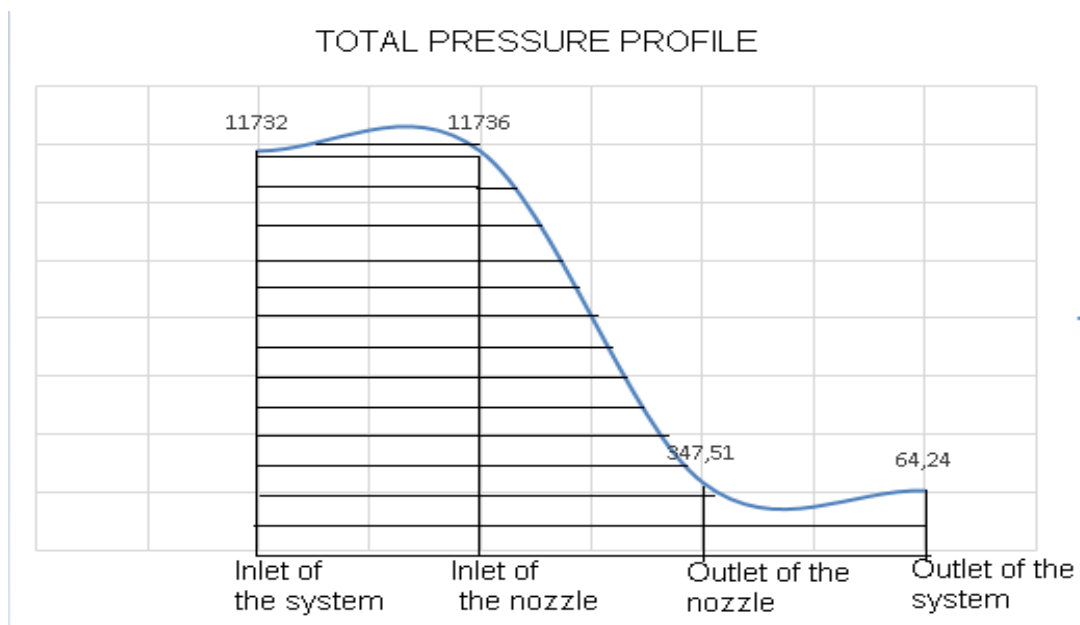


Figure 7.5 Pressure profile graph of grid

### 6.3 Pipe (cylinder) Grid Analysis

The pipe grid is designed as embed pipes in frame and this structure is located on exit of the nozzle.

Again like a normal cylinder grid, we would like to compare both of grid and profiles of velocity, pressure as well. Generally this type grid used to fully develop flow with turbulent condition and produce wakes after passing on cylinder blocks of air.

#### 6.3.1 Model of Pipe Grid

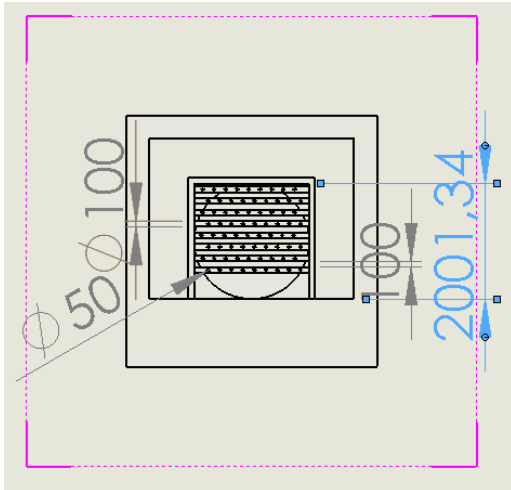


Figure 7.6 Front side of cylinder

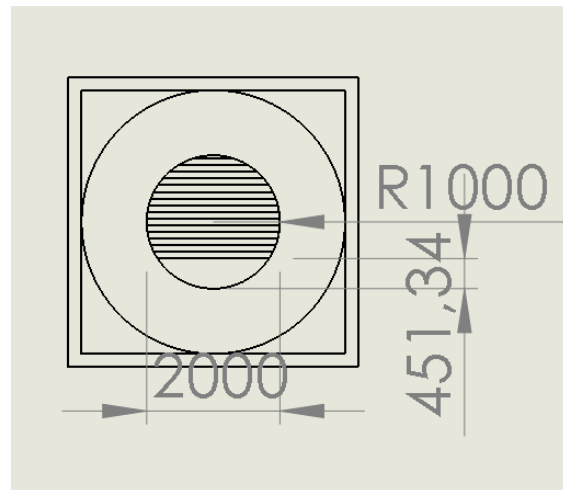


Figure 7.7 back side of cylinder grid

The special cylinder type grid was modelled with 9 horizontal cylinder pipes which was located horizontal at exit of the nozzle and 9x9 cylinder type small pipes were located vertical on the each horizontal cylinder pipes that is facing to inside of the nozzle. Small pipes measurements are 50mm\*50mm and horizontal tall cylinder pipes has 1000mm diameter and length 2000mm height.

#### 6.3.2 Mesh model of the cylinder (pipe) grid

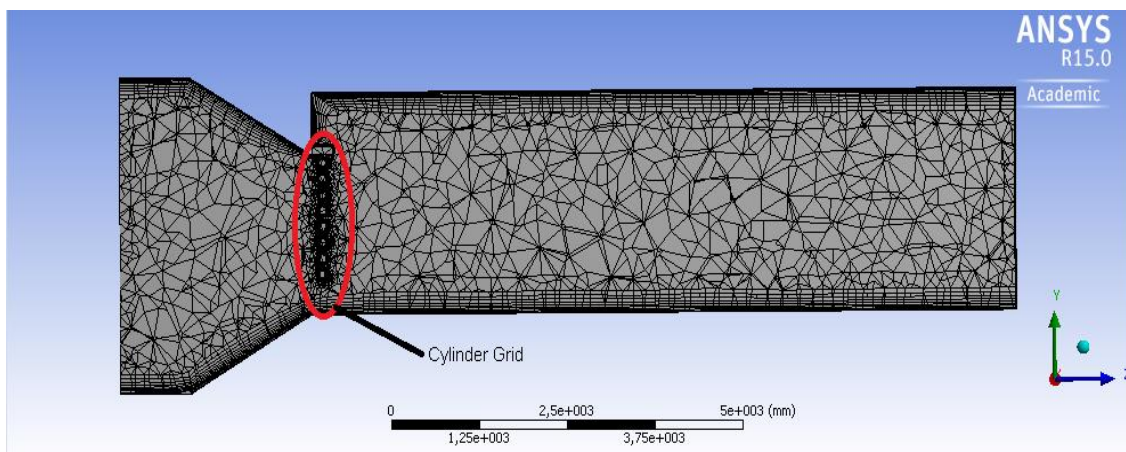


Figure 7.8 Cylinder grid illustration

The meshing of the model with grid, the meshing of the parts is done so that we can brief view of the part we designed and the parameters that we are going to compute in the future using solver as in my case is the velocity. In order to get the good quality which was selected ‘‘Tetrahedrons (Patch Conforming) Method’’ used to reach regular and pure mesh quality.

I try to catch good orthogonal and skewness quality so I applied one operation for the grid.

Statistics	
Bodies	1
Active Bodies	1
Nodes	374374
Elements	881264
Mesh Metric	Orthogonal Quality
Min	0,014165247346078
Max	0,999740895488861
Average	0,83850243317692
Standard Deviation	0,149534645704182

Figure 7.9 Cylinder grid analysis orthogonal

Statistics	
Bodies	1
Active Bodies	1
Nodes	374374
Elements	881264
Mesh Metric	Skewness
Min	1,18029555540444E-03
Max	0,988371193142082
Average	0,307149167484757
Standard Deviation	0,175745592614658

Figure 8 Cylinder grid analysis skewness

Figure 7.9 and 8 show minimum orthogonal quality is  $0.014165 < 0.1$  and maximum skewness quality is  $0.98 > 0.95$ . Very big element size, good orthogonal quality but less skewness quality and tried to catch to perfect values within that element number

### 6.3.3 Fluent Solver

The used of ANSYS fluent solver which was set up as a condition of density based and we use k-epsilon (2 eqn.) for models. Also, our main actor is air as a fluid in the system. Inlet conditions are considered as a boundary condition to analysis to our system.



Reference values for fluent solver respectively;

- Area=1m<sup>2</sup> (which is used to compute the force and moment coefficients)
- Density of Air=1.225 kg/m<sup>3</sup> (compute the reference dynamic pressure)
- Enthalpy=0 (determine the total enthalpy change)
- Length=1m (computation of the moment coefficient)
- Pressure =0 pa (pressure-related forces and moments and the pressure coefficient)
- Temperature=298.15 K (compute entropy for incompressible flows)
- Inlet Velocity of the system=5.5 m/s (calculated by theoretical formula)
- Viscosity=1.7894\*10<sup>-5</sup> (the boundary Reynolds number)
- The ratio of specific heats=1.4

Inlet velocity applied throughout Z direction. Specification method chooses Intensity and Viscosity ratio. Turbulent Intensity is % 5, Turbulent Viscosity ratio is the boundary value for the modified turbulent viscosity,  $\tilde{\nu}$  and by combining  $\frac{\mu_t}{\mu}$  with the appropriate values of density and molecular viscosity which is 10. Wall motion applied as Stationary Wall and Shear condition is no slip. Wall roughness constant shows 0.5.

Solution method;

Scheme	SIMPLE
Gradient	LEAST SQUARES CELL BASED
Pressure	SECOND ORDER
Momentum	SECOND ORDER UPWIND
Turbulent Kinetic Energy	SECOND ORDER UPWIND
Turbulent Dissipation Rate	SECOND ORDER UPWIND

We use implicit solution method as well as calculated 3000 iterations with converged to calculation according to my converge criteria is 10<sup>-6</sup> . Critical locations values were tabulated as inlet of the system, inlet of the nozzle, outlet of the nozzle and outlet of the system as well as element size. 4 tables were prepared to show mean velocities, total pressures, dynamic pressures and absolute pressures

Element size	Inlet Velocity of the system	Inlet Velocity of the nozzle	Outlet Velocity of the nozzle	Outlet velocity of the system
881264	5.5 m/s	7.033288 m/s	27.928326 m/s	8.8901043 m/s

*Table 4.6 Mean velocity results of cylinder grid*

Element Size	Inlet Total Pressure of the system	Inlet Total pressure of the nozzle	Outlet Total pressure of the nozzle	Outlet Total pressure of the system
881264	734.343 pascal	738.123 pascal	734.3075 pascal	78.18998 pascal

Table 4.7 Total pressure results of cylinder grid

Element Size	Inlet Dynamic Pressure of the system	Inlet Dynamic pressure of the nozzle	Outlet Dynamic pressure of the nozzle	Outlet Dynamic pressure of the system
881264	18.542313 pascal	32.609257 pascal	483.80286 pascal	78.965454 pascal

Table 4.8 Dynamic pressure results of cylinder grid

Element Size	Inlet Absolute Pressure of the system	Inlet Absolute pressure of the nozzle	Outlet Absolute pressure of the nozzle	Outlet Absolute pressure of the system
881264	102040.8 pascal	102030.52 pascal	101575.51 pascal	101324.95 pascal

Table 4.9 Absolute pressure results of cylinder grid

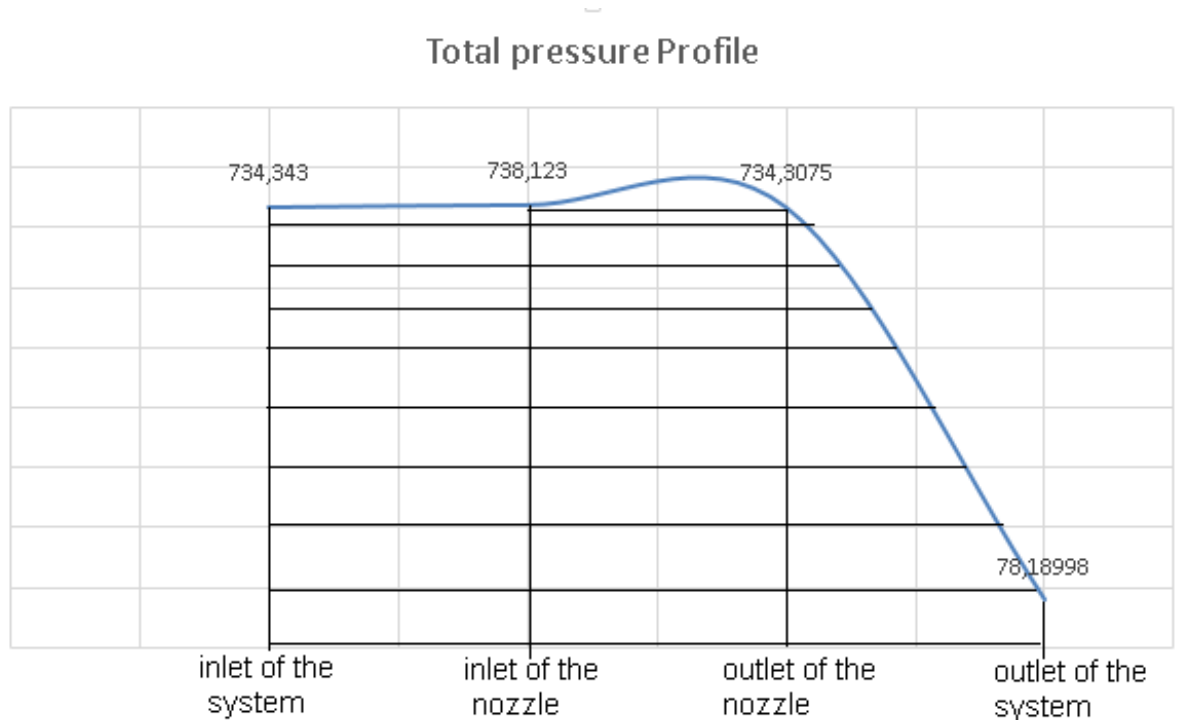


Figure 8.1 Pressure graph of the all system

## RESULTS AND DISCUSSION

First of all Design parameters and theoretical equations were acquired by endowed reference values. The most important reference value is 50 m/s (maximum) where is located at the exit of the nozzle and inlet of the test section at meanwhile. When we followed the Mach number equation, 50 m/s velocity was applied with 20 Celsius air temperature and Mach number calculated 0.145 that means the wind tunnel system was exposed to the subsonic flow. Due to the design of the system, the most important part is nozzle design and De-Laval converged nozzle requisite to provided diversity of air velocity, pressure, density and boundary layers of themselves. The primary conclusions of this study are summarized as follows:

- The hyperbolic curve was discovered by observational investigation of De-Laval converged nozzle's structure that's why hyperbolic equations are used for identification of the De-Laval converged nozzle parameters as inlet, outlet diameters, length of the nozzle. On the other hand inlet and outlet designed cylindrical construction to reach High efficiency as much as non-reversible flow. a and b values represent as the radius of inlet and outlet on the x and y plane. Radii are calculated to the aid of by inlet and outlet area ratio formulation which was combined of Mach number, specific heat ratio within the derivation of motion of equation After that a and b values was substituted qua radii and calculated x and y values were assumed as diameter and length of the nozzle. Inlet, outlet diameters and the nozzle length were determined and results are 1.978meters, 3.956meters, and 1.73 meters respectively. Diameters and length results said that the system has a 0.011 error margin which is suitable and predicted to use for designing the nozzle in addition to this contraction ratio of nozzle calculated as 0.489.
- Also, other important parameters are temperature, pressure and density changes ratio (stagnation properties) at inlet and outlet of the nozzle that ratio equation was provided through a combination of Mach number and specific heat ratio and derivation of the equation of motion. By the way, specific heat ratio is considered the value of 1.4 because of air gets used in the system. Pressure, temperature and density ratio were calculated via specific heat ratio and Mach number, based results show 1.01479, 1.04205 and 1.01054 respectively. As results are shown very close to 1 and it is able to assume no changes in theory and identified an incompressible flow. Formulations of ratio to show regard to compressible flow indeed this research informs every type of flow have property changes and definition of incompressible flow gets used only for theoretical description.
- Velocities at a critical location in the system which is considered mean velocity so required mean velocities are calculated via formulation that is constituted with stagnation properties, enthalpy changes, pressure ratio, temperature difference at inlet and outlet. The exit velocity of the nozzle calculated 26.6 m/s, other critical locations are calculated to aid of the continuity equations, results are 5.5 m/s, 6.9 m/s and 8.45 m/s for inlet of the system, inlet of the nozzle, the outlet of the system respectively.

Necessary turbulent flow demonstrated aid of Reynold's numbers and when mean velocities replaced in the formulation of Reynold's number results are bigger than 4000 for every critical section which is threshold number for turbulent flow. The hydraulic diameter of critical locations where except outlet of the system are considered like directly diameters because these constructions are cylindrical. Comparison of theoretical results of the system with Ansys fluent and Gas dynamic table values gives substantially attestation for a model of the system.

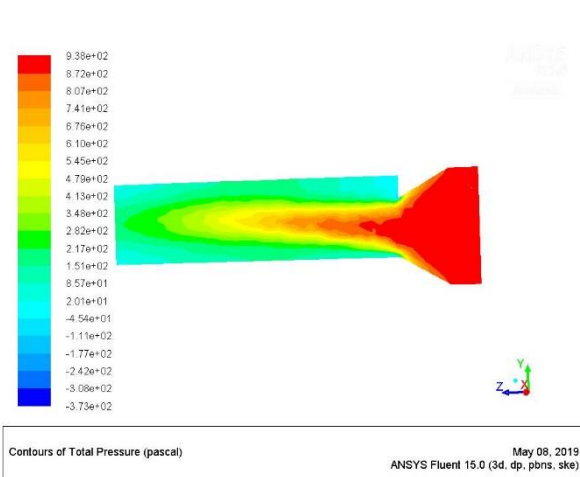


Figure 8.2 Total pressure profile illustration

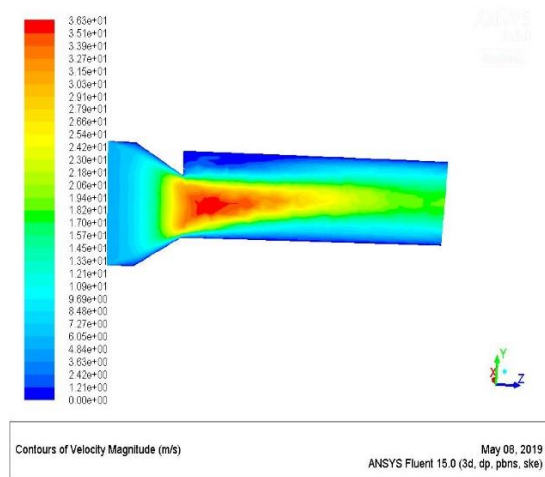


Figure 8.3 Velocity profile illustration

- As we see in figures 8.2 and 8.3 air flow distribution more regular than without grid system and air flow effects dispersion at edges and corners more than without grid system but the system which is assembled grid causes more involve expenses costs like grid material, fan size, etc.

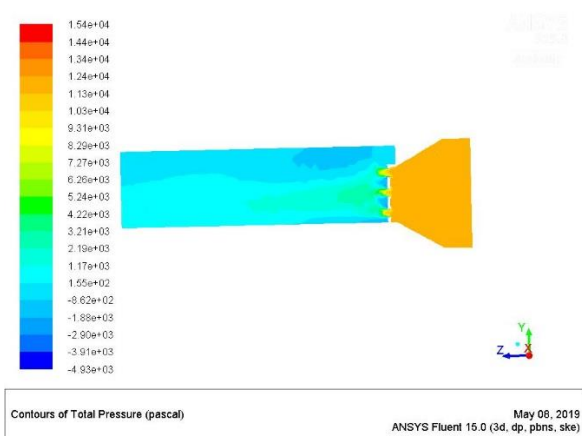


Figure 8.4 Total pressure profile of normal grid

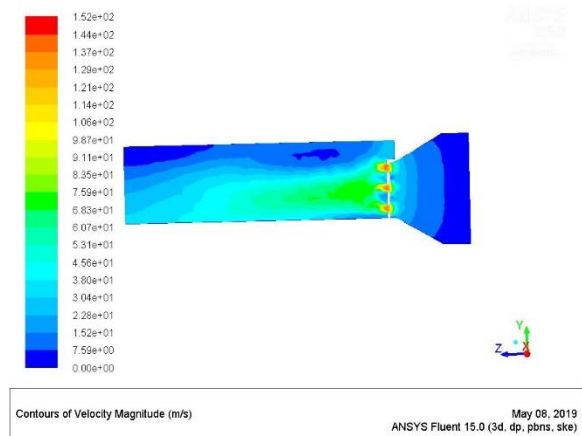


Figure 8.5 Velocity profile of normal grid

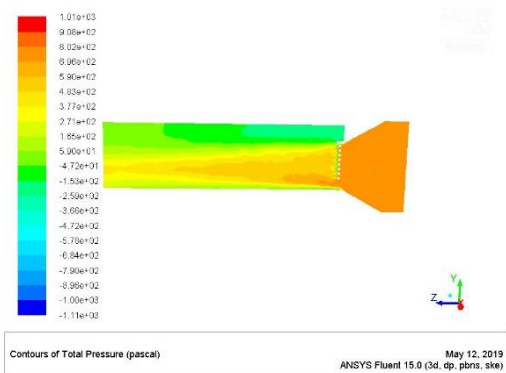


Figure 8.6 Total pressure profile of pipe grid

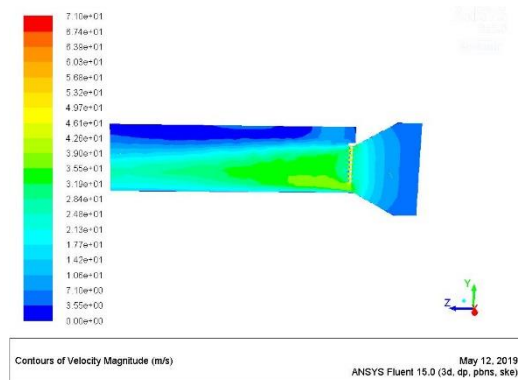


Figure 8.7 Velocity profile of the pipe grid

- When the grids are assembled in figure 8.4, 8.5, 8.6, 8.7 at the outlet of the nozzle and analysis of the system with the grid, we assume low-velocity changes and high pressure increasing and also aim to add the grid in the system is creating more favorable fully developed flow.
- In figure 8.6 and 8.7 we see more regular air flow distribution and less difference pressure than the normal grid and system which is without a grid. As we see below in figure 8.8, 8.9, 9, 9.1, 9.2, 9.3 flow dispersion more efficient in the system which has a cylinder (pipe) grid respectively. The cylinder grid stirred up to preferable dissociation of pressure, velocity, and density where the car is located in the test section and normal grid caused to become unbalanced flow in the system. Cylindrical grid illustrations show suitable average values in the section which is car location.

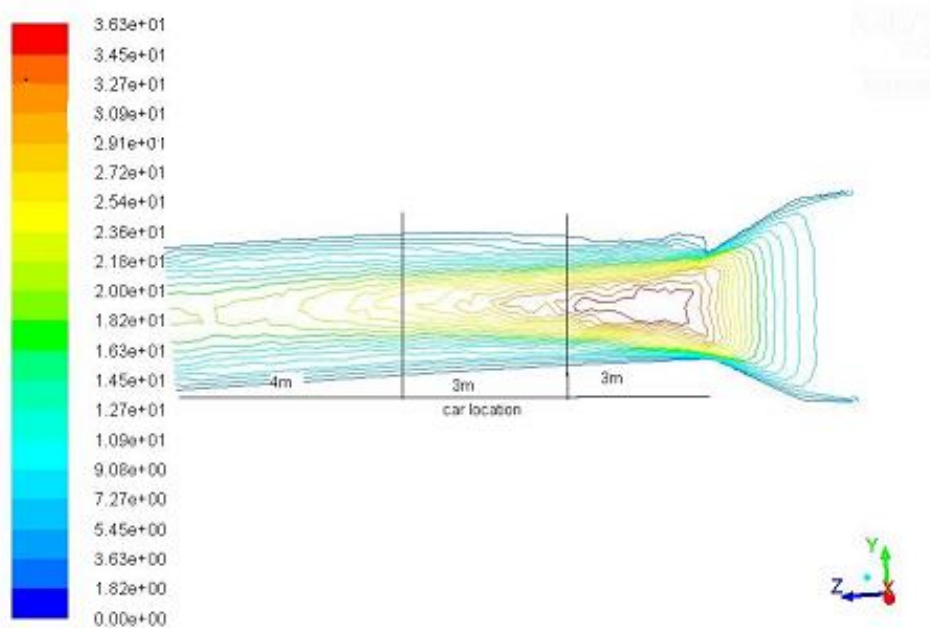


Figure 8.8 car location velocity field without grid

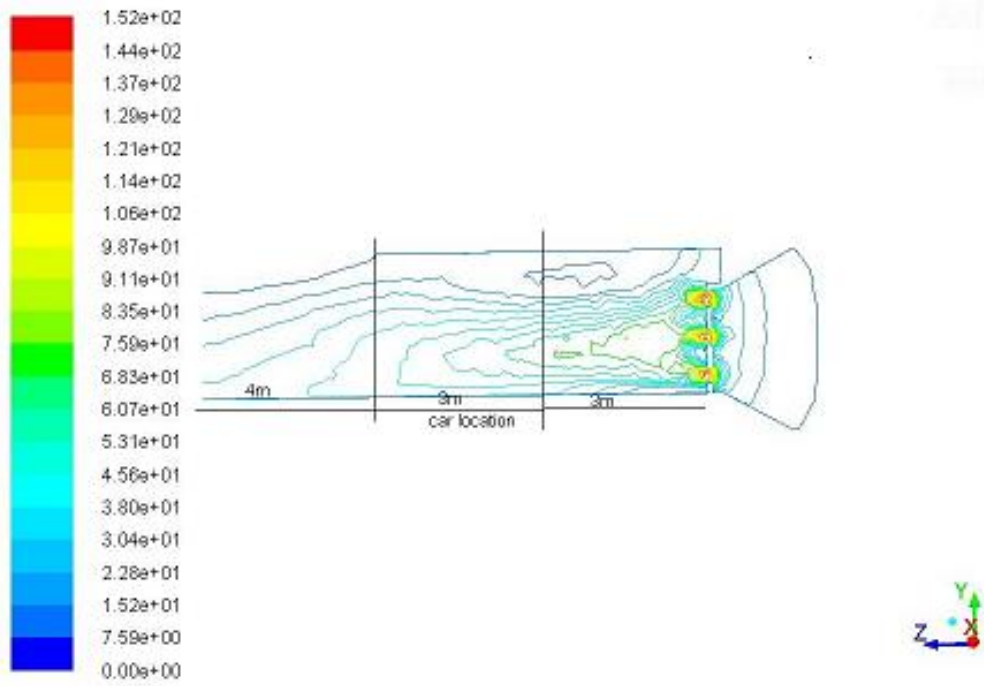


Figure 8.9 car location velocity field of normal grid

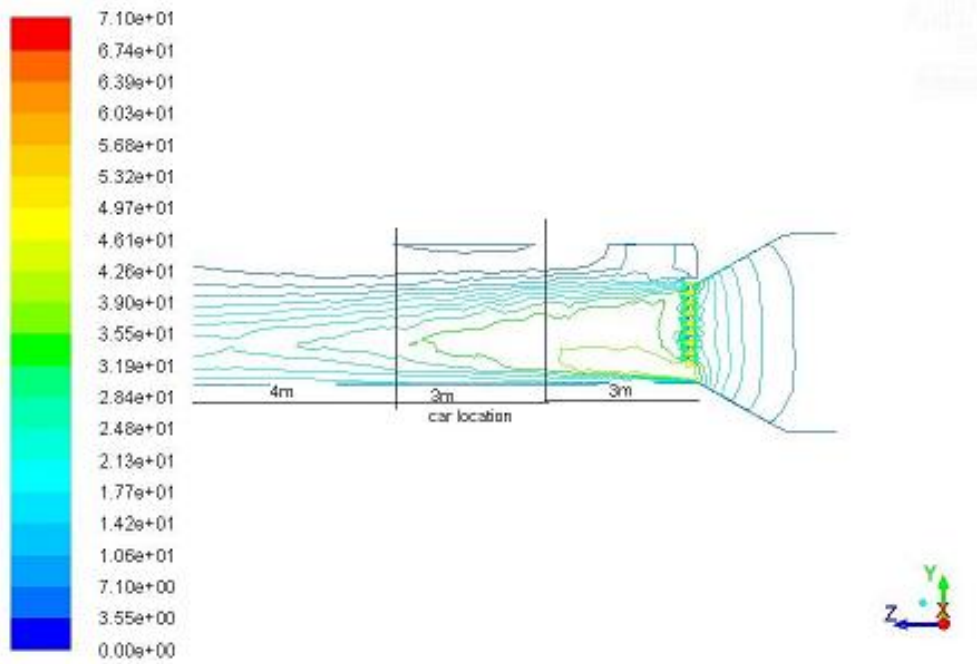


Figure 9 car location velocity field of the pipe grid

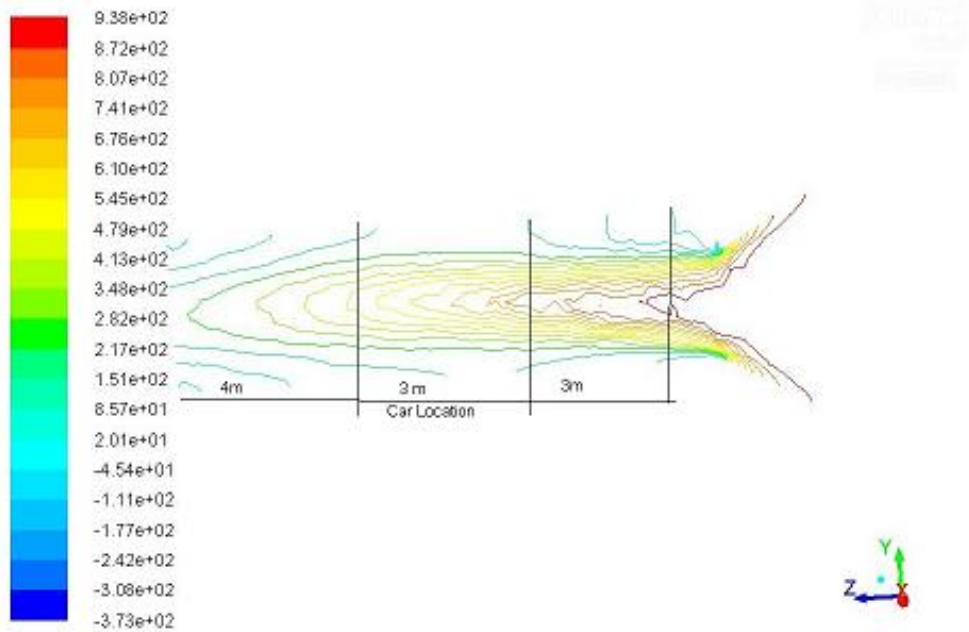


Figure 9.1 car location pressure profile without grid

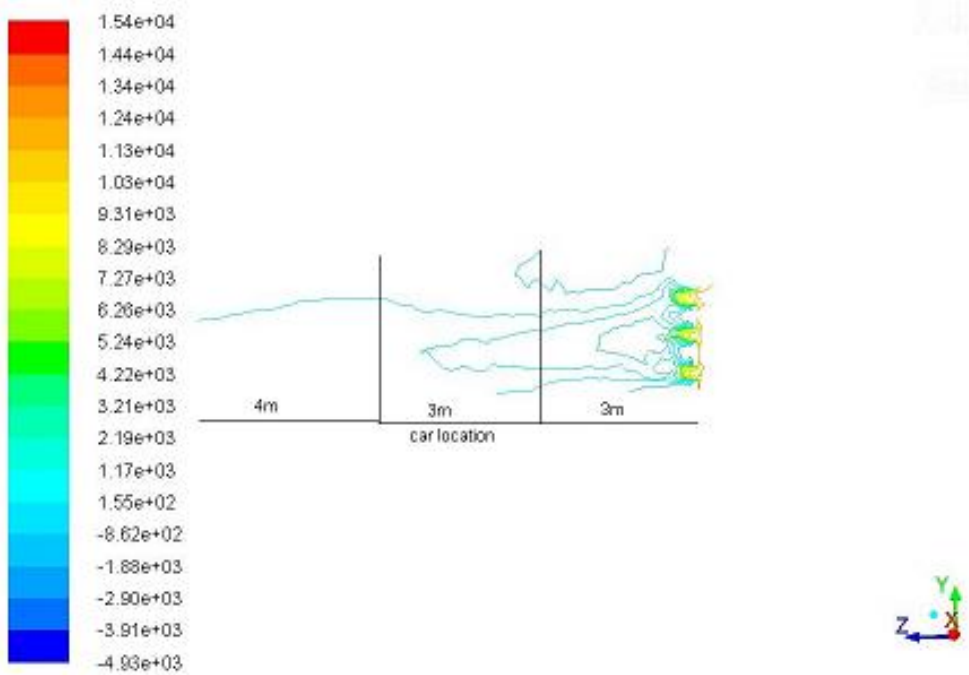


Figure 9.3 car location pressure profile of normal grid

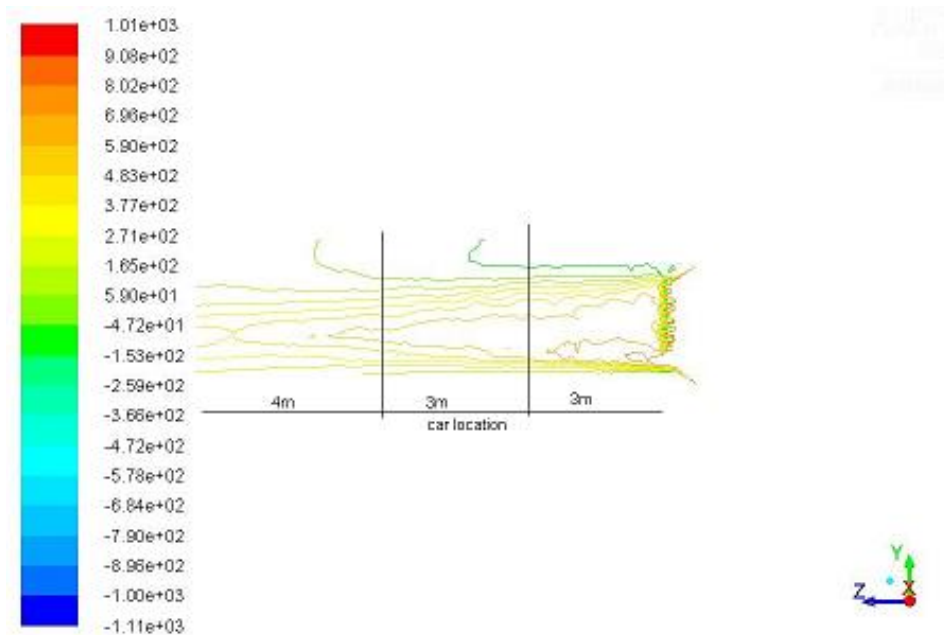


Figure 9.4 car location pressure profile of the pipe grid

- The dandiest condition is resemblance of boundary layers as rain drop because of rain drop was approved the perfect shape of fluid layers. The cylindrical grid catches that similarity within boundary layers in system
- Observed flux density collected in the waist of the test section and very less at corners it is not desirable condition and distribution. In order to reach a fully developed flow with perfect dispersion in the test section, two types of grids are assembled the exit of the nozzle. Grids structure are in titled normal and cylindrical types. Analysis results with grids indicated perfect and better flux density at every point of the test section. However, pressure drop was increased by using grid apparatus. Compare to girds between each other, values and illustrations inferred cylindrical grid more useful than a normal grid. Pressure drop augmentation justification related to Darcy-Welsbach relation that is represented by friction coefficient, length and diameter ratio, mean velocity parameters. In the system, no changes for length, diameter and mean velocity so pressure drop increasing in consideration of friction coefficient rising in the system.



## NOMENCLATURE

<b>Symbol</b>	<b>Meaning</b>
$A_0$	Inlet area
$A^*$	Critical section area
$a$	Substitution Inlet radius
$b$	Substitution Outlet radius
$C$	Speed of sound
$C_p/C_v$	Specific gas constant
$C_f$	Frictional effect
$D$	Diameter
$D_h$	Hydraulic Diameter
$\Delta F$	Frictional Loss
$G$	Gravity
$\Delta H$	Head Loss
$h$	Enthalpy
$k$	Specific heat ratio
$K_l$	Loss coefficient
$M$	Mass
$\dot{m}$	Mass flow rate
$Ma$	Mach number
$n$	Number of mol
$Pe$	Perimeter
$P_r$	Reservoir Pressure
$P$	Pressure
$Re$	Reynold's number
$R$	Gas Constant
$r_0$	Inlet radius
$r_1$	Outlet radius
$r^*$	Critical section radius
$S$	Distance
$T$	Temperature

$\Delta t$	Time derivative
$T_r$	Reservoir Temperature
$\tau_{xx}$	2 dimensional Normal stress on x direction
$U$	Mean Velocity
$U_{xx}$	2 dimensional mean velocity on x direction
$v$	Velocity
$\nu$	Kinematic Viscosity
$xx$	2 dimensional on x direction index
$q$	Density
$Q_{xx}$	2 dimensional Heat Flux on x direction
$x$	Length of nozzle
$y$	Substitution of nozzle diameter
$\Delta w$	Fluid weight loss
$\mu$	Darcy Friction factor
$\gamma$	Dynamic Viscosity

## REFERENCES

- 1-Bar-Meir. (2007). *Gas Dynamic Table*. Retrieved from Potto: [www.potto.org](http://www.potto.org)
- 2-Bauman, N. E. (n.d.). *Heat and Mass Transfer, Fluid engineering*. Moscow, Russia: Russian Academy of Sciences.
- 3-Borgnakke, C. S. (2009). *Fundamentals of Thermodynamics*. Wiley.
- 4-Cantwell. (2015). *Fundamentals of compressible flow*. Retrieved from Stanford: [https://web.stanford.edu/~cantwell/AA210A\\_Course\\_Material/AA210A\\_Course\\_Notes/AA10\\_Fundamentals\\_of\\_Compressible\\_Flow\\_Ch\\_10\\_BJ\\_Cantwell.pdf](https://web.stanford.edu/~cantwell/AA210A_Course_Material/AA210A_Course_Notes/AA10_Fundamentals_of_Compressible_Flow_Ch_10_BJ_Cantwell.pdf)
- 5-Carswell, C. C. (2007). *Principles of Astrophysical Fluid Dynamics*. Cambridge University Press.
- 6-Corliss, D. D. (n.d.). *Wind Tunnels of NASA*. Cleveland, OH 44135: National Aeronautics and Space Administration.
- 7-Ge, C. (2015). *DESIGN, CONSTRUCTION AND CHARACTERIZATION*. New Jersey: New Jersey Institute of Technology.
- 8-Graebel, W. (2001). *Engineering Fluid Mechanics*.
- 9-Hall, N. (2015, May). *NASA*. Retrieved from [grc.nasa.gov](http://grc.nasa.gov): <https://www.grc.nasa.gov/www/k-12/airplane/tuncret.html>
- 10-Hall, N. (n.d.). *Mach Number*. NASA.
- 11-INC., A. (2012, october). *Ansys Fluent tutorial guide*. Canonsburg, PA 15317, The Usa.
- 12-Kestin, J. &. (1962). "The transfer of heat across a turbulent boundary layer at very high prandtl numbers". In *Int. J. Heat Mass Transfer*. (pp. 355-371).
- 13-Konev, V. V. (2001-2009). *Portal*. Retrieved from Tomsk Polytechnic University: [http://portal.tpu.ru:7777/SHARED/k/KONVAL/Sites/English\\_sites/G/c\\_Hyper\\_f.htm](http://portal.tpu.ru:7777/SHARED/k/KONVAL/Sites/English_sites/G/c_Hyper_f.htm)
- 14-Lange, F. M. (n.d.). In *Lange's Handbook of Chemistry* (p. 1524).
- 15-Lockwood, A. (2015, February 11). *Digital Engineering*.
- 16-Miller, J. (2017). *Lumen Learning*. Retrieved from College Algebra: <https://courses.lumenlearning.com/waymakercollegealgebra/chapter/equations-of-hyperbolas/>
- 17-Nakasano, Y. (2006). *Engineering analysis with Ansys software*. Oxford, Burlington.
- 18-Paul, J. C. (1993). *Racing Helmet Design*. Livonia, MI 48150: Airflow Science Corporation.
- 19-Vertical Wind Tunnel. (February, 1945). *Popular Science*, 70-90.
- 20-Yunus A. Çengel, J. M. (2006). *Fluid Mechanics, Fundamentals and applications*. New York: Mc Graw Hill.

- 21- Wiedemann, J. and Potthoff, J., "The New 5-Belt Road Simulation System of the IVK Wind Tunnels - Design and First Results," SAE Technical Paper 2003-01-0429, 2003
- 22- Full-scale Aero-acoustic Wind-tunnel,“ Mitsubishi Heavy Industries, Ltd. Technical Review Vol. 43 No. 3 (Sep. 2006).
- 23- Wickern, G. and Lindener, N., "The Audi Aeroacoustic Wind Tunnel: Final Design and First Operational Experience," SAE Technical Paper 2000-01-0868, 2000,
- 24- H. H. Brouwer, „Anechoic Wind Tunnels,“ National Aerospace Laboratory NLR, 1997, Pages 39 ISSN 0369-478X
- 25- Larose, G., Belluz, L., Whittal, I., Belzile, M. et al., "Evaluation of the Aerodynamics of Drag Reduction Technologies for Light-duty Vehicles: a Comprehensive Wind Tunnel Study," SAE Int. J. Passeng. Cars - Mech. Syst. 9(2):772-784, 2016,
- 26- Forschungsinstitut für Kraftfahrwesen und Fahrzeugmotoren Stuttgart – FKFS, „Magazine for opening the new vehicle wind tunnel at the University of Stuttgart, operated by FKFS Stuttgart – FKFS,“ 2014,
- 27- Schema Tunelu, EPA/4, Ing. Michal Netusil Ph.D., 04.07.2017
- 28- Walter, J., Duell, E., Martindale, B., Arnette, S. et al., "The DaimlerChrysler Full-Scale Aeroacoustic Wind Tunnel," SAE Technical Paper 2003-01-0426, 2003,

## List of Figures

FIGURE 1 OPEN AND CLOSED TYPES OF WIND TUNNEL	3
FIGURE 2 BOUNDARY LAYER REPRESENTATION WITH LAMINAR FLOW AND TURBULENT FLOW	4
FIGURE 2.1 MACH NUMBER REGIMES	9
FIGURE 3 ILLUSTRATION OF HYPERBOLIC EQUATIONS (RIGHT SIDE IS OUR NOZZLE TYPE) (KONEV, 2001-2009)	14
FIGURE 3.1 AREA-MACH NUMBER FUNCTION (CANTWELL, 2015)	18
FIGURE 4 ILLUSTRATION OF HYPERBOLE EQUATION (MILLER, 2017)	25
FIGURE 5 MODEL OF THE WIND TUNNEL SYSTEM	34
FIGURE 5.1 MODEL DETAIL OF THE WIND TUNNEL SYSTEM	34
FIGURE 5.2 TECHNICAL DRAWING OF THE MODEL ON TOP VIEW	35
FIGURE 5.3 TECHNICAL DRAW OF IN FRONT VIEW	35
FIGURE 5.4 TECHNICAL DRAW OF BACK SIDE	35
FIGURE 6 PREPARATION OF ANALYSIS	36
FIGURE 6.1 MESH ILLUSTRATION OF GENERAL SYSTEM	38
FIGURE 6.2 SECTION PLANE SHOWS INFLATION LAYERS OF THE SYSTEM	38
FIGURE 6.3 FIRST APPLICATION ORTHOGONAL QUALITY	39
FIGURE 6.4 FIRST APPLICATION SKEWNESS	39
FIGURE 6.5 SECOND APPLICATION ORTHOGONAL QUALITY	40
FIGURE 6.6 SECOND APPLICATION SKEWNESS	40
FIGURE 6.7 THIRD APPLICATION ORTHOGONAL QUALITY	40
FIGURE 6.8 THIRD APPLICATION SKEWNESS	41
FIGURE 6.9 VELOCITY GRAPH OF OVERALL SYSTEM (M/S)	44
FIGURE 6.9.1 TOTAL PRESSURE GRAPH OF OVERALL SYSTEM (PASCAL)	44
FIGURE 7 FRONT SIDE OF GRID	44
FIGURE 7.1 BACK SIDE OF GRID	45
FIGURE 7.2 GRID ILLUSTRATION WITH INFLATION LAYERS	45
FIGURE 7.3 GRID ANALYSIS ORTHOGONAL QUALITY	46
FIGURE 7.4 GRID ANALYSIS SKEWNESS	46
FIGURE 7.5 PRESSURE PROFILE GRAPH OF GRID	48
FIGURE 7.6 FRONT SIDE OF CYLINDER	49
FIGURE 7.7 BACK SIDE OF CYLINDER GRID	49
FIGURE 7.8 CYLINDER GRID ILLUSTRATION	49
FIGURE 7.9 CYLINDER GRID ANALYSIS ORTHOGONAL	50
FIGURE 8 CYLINDER GRID ANALYSIS SKEWNESS	50
FIGURE 8.1 PRESSURE GRAPH OF THE ALL SYSTEM	52
FIGURE 8.2 TOTAL PRESSURE PROFILE ILLUSTRATION	54
FIGURE 8.3 VELOCITY PROFILE ILLUSTRATION	54
FIGURE 8.4 TOTAL PRESSURE PROFILE OF NORMAL GRID	54
FIGURE 8.5 VELOCITY PROFILE OF NORMAL GRID	54
FIGURE 8.8 CAR LOCATION VELOCITY FIELD WITHOUT GRID	55
FIGURE 8.9 CAR LOCATION VELOCITY FILED OF NORMAL GRID	56
FIGURE 9 CAR LOCATION VELOCITY FIELD OF THE PIPE GRID	56
FIGURE 9.1 CAR LOCATION PRESSURE PROFILE WITHOUT GRID	57
FIGURE 9.3 CAR LOCATION PRESSURE PROFILE OF NORMAL GRID	57
FIGURE 9.4 CAR LOCATION PRESSURE PROFILE OF THE PIPE GRID	58

## List of Tables

TABLE 1 FLOW REGIMES	8
TABLE 2 INITIAL DATA	12
TABLE 3 GIVEN MEASUREMENTS OF THE TEST SECTION	22
TABLE 4 GIVEN AND CONSIDERED VALUES OF THE SYSTEM	23
TABLE 4.1 CALCULATED MEASUREMENTS OF DE-LAVAL NOZZLE	26
TABLE 4.2 GAS DYNAMIC TABLE FOR SUBSONIC	28
TABLE 4.3 GAS DYNAMIC TABLE FOR SUPERSONIC	29
TABLE 4.2 VELOCITY RESULTS OF THE ANALYSIS	42
TABLE 4.3 TOTAL PRESSURE OF THE SYSTEM	42
TABLE 4.4 DYNAMIC PRESSURE OF THE SYSTEM	43
TABLE 4.5 ABSOLUTE PRESSURE OF THE SYSTEM	43
TABLE 4.3 VELOCITY VALUES OF THE GRID SYSTEM	47
TABLE 4.3 TOTAL PRESSURE OF THE GRID SYSTEM	47
TABLE 4.4 DYNAMIC PRESSURE OF THE GRID SYSTEM	48
TABLE 4.5 ABSOLUTE PRESSURE OF GRID SYSTEM	48
TABLE 4.6 VELOCITY RESULTS OF CYLINDER GRID	51
TABLE 4.7 TOTAL PRESSURE RESULTS OF CYLINDER GRID	52
TABLE 4.8 DYNAMIC PRESSURE RESULTS OF CYLINDER GRID	52
TABLE 4.9 ABSOLUTE PRESSURE RESULTS OF CYLINDER GRID	52